

Modelling clusters of galaxies by $f(R)$ -gravity

S. Capozziello, E. De Filippis, V. Salzano

Dipartimento di Scienze Fisiche, Università degli Studi di Napoli Federico II and INFN, Sezione di Napoli, Complesso Universitario di Monte S. Angelo, Via Cinthia, Edificio N, 80126 Napoli, Italy

Accepted xxx, Received yyy; in original form zzz

ABSTRACT

We consider the possibility that masses and gravitational potentials of galaxy cluster, estimated at X-ray wavelengths, could be explained without assuming huge amounts of dark matter, but in the context of $f(R)$ -gravity. Specifically, we take into account the weak field limit of such theories and show that the corrected gravitational potential allows to estimate the total mass of a sample of 12 clusters of galaxies. Results show that such a gravitational potential provides a fair fit to the mass of visible matter (i.e. gas + stars) estimated by X-ray observations, without the need of additional dark matter while the size of the clusters, as already observed at different scale for galaxies, strictly depends on the interaction lengths of the corrections to the Newtonian potential.

Key words: alternative gravity, clusters of galaxies, dark matter, Clusters - X-rays

1 INTRODUCTION

Since the pioneering work by (Zwicky 1933), the problems of high mass-to-light ratios of galaxy clusters and of the rotation curves of spiral galaxies have been faced by asking for huge amounts of unseen matter in the framework of Newtonian theory of gravity. It is interesting to stress the fact that Zwicky addressed such an issue dealing with *missing matter* and not with *dark matter*.

Later on, several versions of the the cold dark matter model (CDM) have been built starting from the assumption that a large amount of non-baryonic matter (i.e. matter non-interacting with the electromagnetic radiation) could account for the observations in the framework of the standard Newtonian dynamics. Besides, by adding a further ingredient, the cosmological constant Λ (Carroll et al. 1992; Sahni & Starobinski 2000), such a model (now Λ CDM) has become the new cosmological paradigm usually called the *concordance model*.

In fact, high quality data coming from the measurements of cluster properties as the mass, the correlation function and the evolution with redshift of their abundance (Eke et al. 1998; Viana et al. 2002; Bahcall et al. 2003; Bahcall & Bode 2003), the Hubble diagram of Type Ia Supernovae (Riess et al. 2004; Astier et al. 2006; Clocchiati et al. 2006), the optical surveys of large scale structure (Pope et al. 2005; Cole et al. 2005; Eisenstein et al. 2005), the anisotropies of the cosmic microwave background (de Bernardis et al. 2000; Spergel et al. 2003), the cosmic shear measured from weak lensing surveys (van Waerbeke et al. 2001; Refregier 2003) and the Lyman- α forest absorption (Croft et al. 1999; Mc-

Donald et al. 2005) are evidences toward a spatially flat universe with a subcritical matter content and undergoing a phase of accelerated expansion. Interpreting all this information in a self-consistent model is the main task of modern cosmology and Λ CDM model provides a good fit to the most of the data (Tegmark et al. 2004; Seljak et al. 2005; Sanchez et al. 2006) giving a reliable snapshot of the today observed universe.

Nevertheless, it is affected by serious theoretical shortcomings that have motivated the search for alternative candidates generically referred to as *dark energy* or *quintessence*. Such models range from scalar fields rolling down self interaction potentials to phantom fields, from phenomenological unified models of dark energy and dark matter to alternative gravity theories (Peebles & Rathra 2003; Padmanabhan 2003; Copeland, Sami, and Tsujikawa 2006).

Essentially, dark energy (or any alternative component) has to act as a negative pressure fluid which gives rise to an overall acceleration of the Hubble fluid. Despite of the clear mechanisms generating the observed cosmological dynamics, the nature and the fundamental properties of dark energy remain essentially unknown notwithstanding the great theoretical efforts made up to now.

The situation for dark matter is similar: its clustering and distribution properties are fairly well known at every scale but its nature is unknown, up to now, at a fundamental level.

On the other hand, the need of unknown components as dark energy and dark matter could be considered nothing else but as a signal of the breakdown of Einstein General

arXiv:0809.1882v1 [astro-ph] 10 Sep 2008

Relativity at astrophysical (galactic and extragalactic) and cosmological scales.

In this context, Extended Theories of Gravity could be, in principle, an interesting alternative to explain cosmic acceleration without any dark energy and large scale structure without any dark matter. In their simplest version, the Ricci curvature scalar R , linear in the Hilbert-Einstein action, could be replaced by a generic function $f(R)$ whose true form could be "reconstructed" by the data. In fact, there is no a priori reason to consider the gravitational Lagrangian linear in the Ricci scalar while observations and experiments could contribute to define and constrain the "true" theory of gravity. For a discussion on this topic, see (Capozziello & Francaviglia 2008; Nojiri & Odintsov 2007; Sotiriou & Faraoni 2008).

In a cosmological framework, such an approach lead to modified Friedmann equations that can be formally written in the usual form by defining an effective *curvature fluid* giving rise to a negative pressure which drives the cosmic acceleration (Capozziello 2002; Capozziello, Carloni and Troisi 2003; Carroll et al. 2004; Capozziello & Francaviglia 2008). Also referred to as $f(R)$ theories, this approach is recently extensively studied both from the theoretical and the observational point of view (see e.g. (Capozziello et al. 2003; Capozziello, Cardone and Francaviglia 2006; Borowiec, Godlowski and Szydowski 2006)). Moreover, this same approach has been also proposed, in early cosmology, as a mechanism giving rise to an inflationary era without the need of any inflaton field (Starobinsky 1980).

All this amount of work has been, essentially, concentrated on the cosmological applications and have convincingly demonstrated that extended theories of gravity (in particular $f(R)$ gravity) are indeed able to explain the cosmic speed up and fairly fit the available data-sets and, hence, represents a viable alternative to the dark energy models (Capozziello, Cardone and Troisi 2005).

Changing the gravity sector could have consequences not only at cosmological scales, but also at the galactic and cluster scales so that it is mandatory to investigate the low energy limit of such theories. A strong debate is open with different results arguing in favor (Dick 2004; Sotiriou 2006; Cembranos 2006; Navarro & van Acoleyen 2005; Allemandi et al. 2005; Capozziello & Troisi 2005) or against (Dolgov & Kawasaki 2003; Chiba 2003; Olmo 2005) such models. It is worth noting that, as a general result, higher order theories of gravity cause the gravitational potential to deviate from its Newtonian $1/r$ scaling (Stelle 1978; Kluske & Schmidt 1996; Schmidt 2004; Clifton & Barrow 2005; Sobouti 2007; Mendoza & Rosas-Guevara 2007) even if such deviations may be vanishing.

In (Capozziello, Cardone and Troisi 2007), the Newtonian limit of power law $f(R) = f_0 R^n$ theories has been investigated, assuming that the metric in the low energy limit ($\Phi/c^2 \ll 1$) may be taken as Schwarzschild-like. It turns out that a power law term $(r/r_c)^\beta$ has to be added to the Newtonian $1/r$ term in order to get the correct gravitational potential. While the parameter β may be expressed analytically as a function of the slope n of the $f(R)$ theory, r_c sets the scale where the correction term starts being significant. A particular range of values of n has been investigated so that the corrective term is an increasing function of the radius r thus causing an increase of the rotation curve with

respect to the Newtonian one and offering the possibility to fit the galaxy rotation curves without the need of further dark matter components.

A set of low surface brightness (LSB) galaxies with extended and well measured rotation curves has been considered (de Blok & Bosma 2002; de Blok 2005). These systems are supposed to be dark matter dominated, and successfully fitting data without dark matter is a strong evidence in favor of the approach (see also (Frigerio Martins & Salucci 2007) for an independent analysis using another sample of galaxies). Combined with the hints coming from the cosmological applications, one should have, in principle, the possibility to address both the dark energy and dark matter problems resorting to the same well motivated fundamental theory (Capozziello, Cardone and Troisi 2006; Koivisto 2007; Lobo 2008). Nevertheless, the simple power law $f(R)$ gravity is nothing else but a toy-model which fail if one tries to achieve a comprehensive model for all the cosmological dynamics, ranging from the early universe, to the large scale structure up to the late accelerated era (Capozziello, Cardone and Troisi 2006; Koivisto 2007).

A fundamental issue is related to clusters and superclusters of galaxies. Such structures, essentially, rule the large scale structure, and are the intermediate step between galaxies and cosmology. As the galaxies, they appear dark-matter dominated but the distribution of dark matter component seems clustered and organized in a very different way with respect to galaxies. It seems that dark matter is ruled by the scale and also its fundamental nature could depend on the scale. For a comprehensive review see (Bahcall 1996).

In the philosophy of Extended Theories of Gravity, the issue is now to reconstruct the mass profile of clusters *without* dark matter, i.e. to find out corrections to the Newton potential producing the same dynamics as dark matter but starting from a well motivated theory. This is the goal of this paper.

As we will see, the problem is very different with respect to that of galaxies and we need different corrections to the gravitational potential in order to consistently fit the cluster mass profiles.

The paper is organized as follows. In Section 2, also referring to other results, we discuss the weak field limit of $f(R)$ -gravity showing that an $f(R)$ theory is, in principle, quite fair to address the cluster problem (Lobo 2008). In Section 3, starting from the corrected potential previously derived for a point-like masses, we generalize the results to extended spherically symmetric systems as required for well shaped cluster models of the Bautz and Morgan classification (Bautz 1970). Section 4 is devoted to the description of the general properties of galaxy clusters. In Section 5, the sample of galaxy clusters which we are going to fit is discussed in details. Results are presented in Section 6, while Section 7 is devoted to the discussion and the conclusions.

2 $F(R)$ -GRAVITY

Let us consider the general action :

$$\mathcal{A} = \int d^4x \sqrt{-g} [f(R) + \mathcal{X}\mathcal{L}_m], \quad (1)$$

where $f(R)$ is an analytic function of the Ricci scalar R , g is the determinant of the metric $g_{\mu\nu}$, $\mathcal{X} = \frac{16\pi G}{c^4}$ is the coupling constant and \mathcal{L}_m is the standard perfect-fluid matter Lagrangian. Such an action is the straightforward generalization of the Hilbert-Einstein action of GR obtained for $f(R) = R$. Since we are considering the metric approach, field equations are obtained by varying (1) with respect to the metric :

$$f' R_{\mu\nu} - \frac{1}{2} f g_{\mu\nu} - f'_{;\mu\nu} + g_{\mu\nu} \square f' = \frac{\mathcal{X}}{2} T_{\mu\nu}. \quad (2)$$

where $T_{\mu\nu} = \frac{-2}{\sqrt{-g}} \frac{\delta(\sqrt{-g}\mathcal{L}_m)}{\delta g^{\mu\nu}}$ is the energy momentum tensor of matter, the prime indicates the derivative with respect to R and $\square = \cdot_{;\sigma}{}^{\sigma}$. We adopt the signature $(+, -, -, -)$.

As discussed in details in (Capozziello, Stabile and Troisi 2008a), we deal with the Newtonian and the post-Newtonian limit of $f(R)$ - gravity on a spherically symmetric background. Solutions for the field equations can be obtained by imposing the spherical symmetry (Capozziello, Stabile and Troisi 2007b):

$$ds^2 = g_{00}(x^0, r) dx^{0^2} + g_{rr}(x^0, r) dr^2 - r^2 d\Omega \quad (3)$$

where $x^0 = ct$ and $d\Omega$ is the angular element.

To develop the post-Newtonian limit of the theory, one can consider a perturbed metric with respect to a Minkowski background $g_{\mu\nu} = \eta_{\mu\nu} + h_{\mu\nu}$. The metric coefficients can be developed as:

$$\begin{cases} g_{tt}(t, r) \simeq 1 + g_{tt}^{(2)}(t, r) + g_{tt}^{(4)}(t, r) \\ g_{rr}(t, r) \simeq -1 + g_{rr}^{(2)}(t, r) \\ g_{\theta\theta}(t, r) = -r^2 \\ g_{\phi\phi}(t, r) = -r^2 \sin^2 \theta \end{cases}, \quad (4)$$

where we put, for the sake of simplicity, $c = 1$, $x^0 = ct \rightarrow t$. We want to obtain the most general result without imposing particular forms for the $f(R)$ -Lagrangian. We only consider analytic Taylor expandable functions

$$f(R) \simeq f_0 + f_1 R + f_2 R^2 + f_3 R^3 + \dots \quad (5)$$

To obtain the post-Newtonian approximation of $f(R)$ - gravity, one has to plug the expansions (4) and (5) into the field equations (2) and then expand the system up to the orders $O(0)$, $O(2)$ and $O(4)$. This approach provides general results and specific (analytic) Lagrangians are selected by the coefficients f_i in (5) (Capozziello, Stabile and Troisi 2008a).

If we now consider the $O(2)$ - order of approximation, the field equations (2), in the vacuum case, results to be

$$\begin{cases} f_1 r R^{(2)} - 2f_1 g_{tt,r}^{(2)} + 8f_2 R_{,r}^{(2)} - f_1 r g_{tt,rr}^{(2)} + 4f_2 r R^{(2)} = 0 \\ f_1 r R^{(2)} - 2f_1 g_{rr,r}^{(2)} + 8f_2 R_{,r}^{(2)} - f_1 r g_{rr,rr}^{(2)} = 0 \\ 2f_1 g_{rr}^{(2)} - r[f_1 r R^{(2)} \\ - f_1 g_{tt,r}^{(2)} - f_1 g_{rr,r}^{(2)} + 4f_2 R_{,r}^{(2)} + 4f_2 r R_{,rr}^{(2)}] = 0 \\ f_1 r R^{(2)} + 6f_2 [2R_{,r}^{(2)} + r R_{,rr}^{(2)}] = 0 \\ 2g_{rr}^{(2)} + r[2g_{tt,r}^{(2)} - r R^{(2)} + 2g_{rr,r}^{(2)} + r g_{rr,rr}^{(2)}] = 0 \end{cases} \quad (6)$$

It is evident that the trace equation (the fourth in the system (6)), provides a differential equation with respect to the Ricci scalar which allows to solve the system at $O(2)$ - order. One obtains the general solution :

$$\begin{cases} g_{tt}^{(2)} = \delta_0 - \frac{2GM}{f_1 r} - \frac{\delta_1(t) e^{-r\sqrt{-\xi}}}{3\xi r} + \frac{\delta_2(t) e^{r\sqrt{-\xi}}}{6(-\xi)^{3/2} r} \\ g_{rr}^{(2)} = -\frac{2GM}{f_1 r} + \frac{\delta_1(t)[r\sqrt{-\xi}+1]e^{-r\sqrt{-\xi}}}{3\xi r} - \frac{\delta_2(t)[\xi r + \sqrt{-\xi}]e^{r\sqrt{-\xi}}}{6\xi^2 r} \\ R^{(2)} = \frac{\delta_1(t) e^{-r\sqrt{-\xi}}}{r} - \frac{\delta_2(t) \sqrt{-\xi} e^{r\sqrt{-\xi}}}{2\xi r} \end{cases} \quad (7)$$

where $\xi \doteq \frac{f_1}{6f_2}$, f_1 and f_2 are the expansion coefficients obtained by the $f(R)$ -Taylor series. In the limit $f \rightarrow R$, for a point-like source of mass M we recover the standard Schwarzschild solution. Let us notice that the integration constant δ_0 is dimensionless, while the two arbitrary time-functions $\delta_1(t)$ and $\delta_2(t)$ have respectively the dimensions of $length^{-1}$ and $length^{-2}$; ξ has the dimension $length^{-2}$. As extensively discussed in (Capozziello, Stabile and Troisi 2008a), the functions $\delta_i(t)$ ($i = 1, 2$) are completely arbitrary since the differential equation system (6) depends only on spatial derivatives. Besides, the integration constant δ_0 can be set to zero, as in the standard theory of potential, since it represents an unessential additive quantity. In order to obtain the physical prescription of the asymptotic flatness at infinity, we can discard the Yukawa growing mode in (7) and then the metric is :

$$\begin{aligned} ds^2 &= \left[1 - \frac{2GM}{f_1 r} - \frac{\delta_1(t) e^{-r\sqrt{-\xi}}}{3\xi r} \right] dt^2 \\ &- \left[1 + \frac{2GM}{f_1 r} - \frac{\delta_1(t)(r\sqrt{-\xi}+1)e^{-r\sqrt{-\xi}}}{3\xi r} \right] dr^2 \\ &- r^2 d\Omega. \end{aligned} \quad (8)$$

The Ricci scalar curvature is

$$R = \frac{\delta_1(t) e^{-r\sqrt{-\xi}}}{r}. \quad (9)$$

The solution can be given also in terms of gravitational potential. In particular, we have an explicit Newtonian-like term into the definition. The first of (7) provides the second order solution in term of the metric expansion (see the definition (4)). In particular, it is $g_{tt} = 1 + 2\phi_{grav} = 1 + g_{tt}^{(2)}$ and then the gravitational potential of an analytic $f(R)$ -theory is

$$\phi_{grav} = -\frac{GM}{f_1 r} - \frac{\delta_1(t) e^{-r\sqrt{-\xi}}}{6\xi r}. \quad (10)$$

Among the possible analytic $f(R)$ -models, let us consider the Taylor expansion where the cosmological term (the above f_0) and terms higher than second have been discarded. We rewrite the Lagrangian (5) as

$$f(R) \sim a_1 R + a_2 R^2 + \dots \quad (11)$$

and specify the above gravitational potential (10), generated by a point-like matter distribution, as:

$$\phi(r) = -\frac{3GM}{4a_1 r} \left(1 + \frac{1}{3} e^{-\frac{r}{L}}\right), \quad (12)$$

where

$$L \equiv L(a_1, a_2) = \left(-\frac{6a_2}{a_1}\right)^{1/2}. \quad (13)$$

L can be defined as the *interaction length* of the problem* due to the correction to the Newtonian potential. We have changed the notation to remark that we are doing only a specific choice in the wide class of potentials (10), but the following considerations are completely general.

3 EXTENDED SYSTEMS

The gravitational potential (12) is a point-like one. Now we have to generalize this solution to extended systems. Let us describe galaxy clusters as spherically symmetric systems and then we have to extend the above considerations to this geometrical configuration. We simply consider the system composed by many infinitesimal mass elements dm each one contributing with a point-like gravitational potential. Then, summing up all terms, namely integrating them on a spherical volume, we obtain a suitable potential. Specifically, we have to solve the integral:

$$\Phi(r) = \int_0^\infty r'^2 dr' \int_0^\pi \sin \theta' d\theta' \int_0^{2\pi} d\omega' \phi(r'). \quad (14)$$

The point-like potential (12) can be split in two terms. The *Newtonian* component is

$$\phi_N(r) = -\frac{3GM}{4a_1 r} \quad (15)$$

The extended integral of such a part is well-known (apart from the numerical constant $\frac{3}{4a_1}$) expression. It is

$$\Phi_N(r) = -\frac{3}{4a_1} \frac{GM(<r)}{r} \quad (16)$$

where $M(<r)$ is the mass enclosed in a sphere with radius r . The *correction* term

$$\phi_C(r) = -\frac{GM}{4a_1} \frac{e^{-\frac{r}{L}}}{r} \quad (17)$$

considering some analytical steps in the integration of the angular part, give the expression

* Such a length is function of the series coefficients, a_1 and a_2 , and it is not a free independent parameter in the following fit procedure.

$$\Phi_C(r) = -\frac{2\pi G}{4} \cdot L \int_0^\infty dr' r' \rho(r') \cdot \frac{e^{-\frac{|r-r'|}{L}} - e^{-\frac{|r+r'|}{L}}}{r} \quad (18)$$

The radial integral is numerically estimated once the mass density is given. We underline a fundamental difference between such a term and the Newtonian one: while in the latter, the matter outside the spherical shell of radius r does not contribute to the potential, in the former, external matter takes part to the integration procedure. For this reason we split the corrective potential in two terms:

- if $r' < r$:

$$\begin{aligned} \Phi_{C,int}(r) &= -\frac{2\pi G}{4} \cdot L \int_0^r dr' r' \rho(r') \cdot \frac{e^{-\frac{|r-r'|}{L}} - e^{-\frac{|r+r'|}{L}}}{r} \\ &= -\frac{2\pi G}{4} \cdot L \int_0^r dr' r' \rho(r') \cdot e^{-\frac{r+r'}{L}} \left(\frac{-1 + e^{\frac{2r'}{L}}}{r} \right) \end{aligned}$$

- if $r' > r$:

$$\begin{aligned} \Phi_{C,ext}(r) &= -\frac{2\pi G}{4} \cdot L \int_r^\infty dr' r' \rho(r') \cdot \frac{e^{-\frac{|r-r'|}{L}} - e^{-\frac{|r+r'|}{L}}}{r} = \\ &= -\frac{2\pi G}{4} \cdot L \int_r^\infty dr' r' \rho(r') \cdot e^{-\frac{r+r'}{L}} \left(\frac{-1 + e^{\frac{2r'}{L}}}{r} \right) \end{aligned}$$

The total potential of the spherical mass distribution will be

$$\Phi(r) = \Phi_N(r) + \Phi_{C,int}(r) + \Phi_{C,ext}(r) \quad (19)$$

As we will show below, for our purpose, we need the gravitational potential derivative with respect to the variable r ; the two derivatives may not be evaluated analytically so we estimate them numerically, once we have given an expression for the *total* mass density $\rho(r)$. While the Newtonian term gives the simple expression:

$$-\frac{d\Phi_N}{dr}(r) = -\frac{3}{4a_1} \frac{GM(<r)}{r^2} \quad (20)$$

the internal and external derivatives of the corrective potential terms are more involved. We do not give them explicitly for sake of brevity, but they are integral-functions of the form

$$\mathcal{F}(r, r') = \int_{\alpha(r)}^{\beta(r)} dr' f(r, r') \quad (21)$$

from which one has:

$$\begin{aligned} \frac{d\mathcal{F}(r, r')}{dr} &= \int_{\alpha(r)}^{\beta(r)} dr' \frac{df(r, r')}{dr} + \\ &- f(r, \alpha(r)) \frac{d\alpha}{dr}(r) + f(r, \beta(r)) \frac{d\beta}{dr}(r) \end{aligned} \quad (22)$$

Such an expression is numerically derived once the integration extremes are given. A general consideration is in order at this point. Clearly, the Gauss theorem holds only for the Newtonian part since, for this term, the force law scales as $1/r^2$. For the total potential (12), it does not hold anymore due to the correction. From a physical point of view, this is not a problem because the full conservation laws are determined, for $f(R)$ -gravity, by the contracted Bianchi identities which assure the self-consistency. For a detailed discussion, see (Capozziello, Cardone and Troisi 2007; Capozziello & Francaviglia 2008; Sotiriou & Faraoni 2008).

4 CLUSTER MASS PROFILES

Clusters of galaxies are generally considered self-bound gravitational systems with spherical symmetry and in hydrostatic equilibrium if virialized. The last two hypothesis are still widely used, despite of the fact that it has been widely proved that most clusters show more complex morphologies and/or signs of strong interactions or dynamical activity, especially in their innermost regions (Chakrabarty et al. 2008; De Filippis et al. 2005).

Under the hypothesis of spherical symmetry in hydrostatic equilibrium, the structure equation can be derived from the collisionless Boltzmann equation

$$\frac{d}{dr}(\rho_{gas}(r) \sigma_r^2) + \frac{2\rho_{gas}(r)}{r}(\sigma_r^2 - \sigma_{\theta,\omega}^2) = -\rho_{gas}(r) \cdot \frac{d\Phi(r)}{dr} \quad (23)$$

where Φ is the gravitational potential of the cluster, σ_r and $\sigma_{\theta,\omega}$ are the mass-weighted velocity dispersions in the radial and tangential directions, respectively, and ρ is gas mass-density. For an isotropic system, it is

$$\sigma_r = \sigma_{\theta,\omega} \quad (24)$$

The pressure profile can be related to these quantities by

$$P(r) = \sigma_r^2 \rho_{gas}(r) \quad (25)$$

Substituting Eqs. (24) and (25) into Eq. (23), we have, for an isotropic sphere,

$$\frac{dP(r)}{dr} = -\rho_{gas}(r) \frac{d\Phi(r)}{dr} \quad (26)$$

For a gas sphere with temperature profile $T(r)$, the velocity dispersion becomes

$$\sigma_r^2 = \frac{kT(r)}{\mu m_p} \quad (27)$$

where k is the Boltzmann constant, $\mu \approx 0.609$ is the mean mass particle and m_p is the proton mass. Substituting Eqs. (25) and (27) into Eq. (26), we obtain

$$\frac{d}{dr} \left(\frac{kT(r)}{\mu m_p} \rho_{gas}(r) \right) = -\rho_{gas}(r) \frac{d\Phi}{dr}$$

or, equivalently,

$$-\frac{d\Phi}{dr} = \frac{kT(r)}{\mu m_p r} \left[\frac{d \ln \rho_{gas}(r)}{d \ln r} + \frac{d \ln T(r)}{d \ln r} \right] \quad (28)$$

Now the total gravitational potential of the cluster is:

$$\Phi(r) = \Phi_N(r) + \Phi_C(r) \quad (29)$$

with

$$\Phi_C(r) = \Phi_{C,int}(r) + \Phi_{C,ext}(r) \quad (30)$$

It is worth underlining that if we consider *only* the standard Newtonian potential, the *total* cluster mass $M_{cl,N}(r)$ is composed by gas mass + mass of galaxies + cD-galaxy mass + dark matter and it is given by the expression:

$$\begin{aligned} M_{cl,N}(r) &= M_{gas}(r) + M_{gal}(r) + M_{CDgal}(r) + M_{DM}(r) \\ &= -\frac{kT(r)}{\mu m_p G} r \left[\frac{d \ln \rho_{gas}(r)}{d \ln r} + \frac{d \ln T(r)}{d \ln r} \right] \end{aligned} \quad (31)$$

$M_{cl,N}$ means the standard estimated *Newtonian* mass. Generally the galaxy part contribution is considered negligible with respect to the other two components so we have:

$$\begin{aligned} M_{cl,N}(r) &\approx M_{gas}(r) + M_{DM}(r) \approx \\ &\approx -\frac{kT(r)}{\mu m_p} r \left[\frac{d \ln \rho_{gas}(r)}{d \ln r} + \frac{d \ln T(r)}{d \ln r} \right] \end{aligned}$$

Since the gas-mass estimates are provided by X-ray observations, the equilibrium equation can be used to derive the amount of dark matter present in a cluster of galaxies and its spatial distribution.

Inserting the previously defined *extended-corrected* potential of Eq. (29) into Eq. (28), we obtain:

$$-\frac{d\Phi_N}{dr} - \frac{d\Phi_C}{dr} = \frac{kT(r)}{\mu m_p r} \left[\frac{d \ln \rho_{gas}(r)}{d \ln r} + \frac{d \ln T(r)}{d \ln r} \right] \quad (32)$$

from which the *extended-corrected* mass estimate follows:

$$\begin{aligned} M_{cl,EC}(r) + \frac{4a_1}{3G} r^2 \frac{d\Phi_C}{dr}(r) &= \\ &= \frac{4a_1}{3} \left[-\frac{kT(r)}{\mu m_p G} r \left(\frac{d \ln \rho_{gas}(r)}{d \ln r} + \frac{d \ln T(r)}{d \ln r} \right) \right] \end{aligned} \quad (33)$$

Since the use of a corrected potential avoids, in principle, the additional requirement of dark matter, the total cluster mass, in this case, is given by:

$$M_{cl,EC}(r) = M_{gas}(r) + M_{gal}(r) + M_{CDgal}(r) \quad (34)$$

and the mass density in the Φ_C term is

$$\rho_{cl,EC}(r) = \rho_{gas}(r) + \rho_{gal}(r) + \rho_{CDgal}(r) \quad (35)$$

with the density components derived from observations.

In this work, we will use Eq. (33) to compare the anionic mass profile $M_{cl,EC}(r)$, estimated from observations, with the theoretical deviation from the Newtonian gravitational potential, given by the expression $-\frac{4a_1}{3G} r^2 \frac{d\Phi_C}{dr}(r)$. Our goal is to reproduce the observed mass profiles for a sample of galaxy clusters.

5 GALAXY CLUSTER SAMPLE

The formalism described in § 4 can be applied to a sample of 12 galaxy clusters. We shall use the cluster sample studied in (Vikhlinin et al.2005; Vikhlinin et al.2006) which consists of 13 low-redshift clusters spanning a temperature range $0.7 \div 9.0$ keV derived from high quality *Chandra* archival data. In all these clusters, the surface brightness and the gas temperature profiles are measured out to large radii, so that mass estimates can be extended up to r_{500} or beyond.

5.1 Gas Density Model

The gas density distribution of the clusters in the sample is described by the analytic model proposed in (Vikhlinin et al.2006). Such a model modifies the classical β -model to represent the characteristic properties of the observed X-ray surface brightness profiles, i.e. the power-law-type cusps of gas density in the cluster center, instead of a flat core and the steepening of the brightness profiles at large radii. Eventually, a second β -model, with a small core radius, is added to improve the model close to the cluster cores. The analytical form for the particle emission is given by:

$$n_p n_e = n_0^2 \cdot \frac{(r/r_c)^{-\alpha}}{(1+r^2/r_c^2)^{3\beta-\alpha/2}} \cdot \frac{1}{(1+r^\gamma/r_s^2)^{\epsilon/\gamma}} +$$

$$+ \frac{n_{02}^2}{(1 + r^2/r_{c2}^2)^{3\beta_2}} \quad (36)$$

which can be easily converted to a mass density using the relation:

$$\rho_{gas} = n_T \cdot \mu m_p = \frac{1.4}{1.2} n_e m_p \quad (37)$$

where n_T is the total number density of particles in the gas. The resulting model has a large number of parameters, some of which do not have a direct physical interpretation. While this can often be inappropriate and computationally inconvenient, it suits well our case, where the main requirement is a detailed qualitative description of the cluster profiles.

In (Vikhlinin et al.2006), Eq. (36) is applied to a restricted range of distances from the cluster center, i.e. between an inner cutoff r_{min} , chosen to exclude the central temperature bin ($\approx 10 \div 20$ kpc) where the ICM is likely to be multi-phase, and r_{det} , where the X-ray surface brightness is at least 3σ significant. We have extrapolated the above function to values outside this restricted range using the following criteria:

- for $r < r_{min}$, we have performed a linear extrapolation of the first three terms out to $r = 0$ kpc;
- for $r > r_{det}$, we have performed a linear extrapolation of the last three terms out to a distance \bar{r} for which $\rho_{gas}(\bar{r}) = \rho_c$, ρ_c being the critical density of the Universe at the cluster redshift: $\rho_c = \rho_{c,0} \cdot (1+z)^3$. For radii larger than \bar{r} , the gas density is assumed constant at $\rho_{gas}(\bar{r})$.

We point out that, in Table 1, the radius limit r_{min} is almost the same as given in the previous definition. When the value given by (Vikhlinin et al.2006) is less than the cD-galaxy radius, which is defined in the next section, we choose this last one as the lower limit. On the contrary, r_{max} is quite different from r_{det} : it is fixed by considering the higher value of temperature profile and not by imaging methods.

We then compute the gas mass $M_{gas}(r)$ and the total mass $M_{cl,N}(r)$, respectively, for all clusters in our sample, substituting Eq. (36) into Eqs. (37) and (31), respectively; the gas temperature profile is described in details in § 5.2. The resulting mass values, estimated at $r = r_{max}$, are listed in Table 1.

5.2 Temperature Profiles

As stressed in § 5.1, for the purpose of this work, we need an accurate qualitative description of the radial behavior of the gas properties. Standard isothermal or polytropic models, or even the more complex one proposed in (Vikhlinin et al.2006), do not provide a good description of the data at all radii and for all clusters in the present sample. We hence describe the gas temperature profiles using the straightforward X-ray spectral analysis results, without the introduction of any analytic model.

X-ray spectral values have been provided by A. Vikhlinin (private communication). A detailed description of the relative spectral analysis can be found in (Vikhlinin et al.2005).

5.3 Galaxy Distribution Model

The galaxy density can be modelled as proposed by (Bahcall 1996). Even if the galaxy distribution is a *point*-distribution

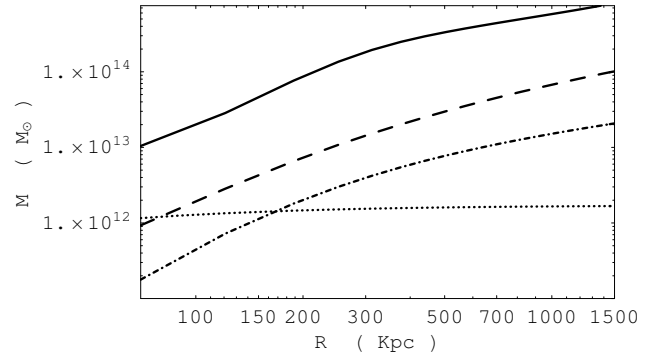


Figure 1. Matter components for A478: total Newtonian dynamical mass (continue line); gas mass (dashed line); galactic mass (dotted-dashed line); cD-galaxy mass (dotted line).

instead of a continuous function, assuming that galaxies are in equilibrium with gas, we can use a β -model, $\propto r^{-3}$, for $r < R_c$ from the cluster center, and a steeper one, $\propto r^{-2.6}$, for $r > R_c$, where R_c is the cluster core radius (its value is taken from Vikhlinin 2006). Its final expression is:

$$\rho_{gal}(r) = \begin{cases} \rho_{gal,1} \cdot \left[1 + \left(\frac{r}{R_c}\right)^2\right]^{-\frac{3}{2}} & r < R_c \\ \rho_{gal,2} \cdot \left[1 + \left(\frac{r}{R_c}\right)^2\right]^{-\frac{2.6}{2}} & r > R_c \end{cases} \quad (38)$$

where the constants $\rho_{gal,1}$ and $\rho_{gal,2}$ are chosen in the following way:

- (Bahcall 1996) provides the central number density of galaxies in rich compact clusters for galaxies located within a $1.5 h^{-1} \text{Mpc}$ radius from the cluster center and brighter than $m_3 + 2^m$ (where m_3 is the magnitude of the third brightest galaxy): $n_{gal,0} \sim 10^3 h^3 \text{ galaxies Mpc}^{-3}$. Then we fix $\rho_{gal,1}$ in the range $\sim 10^{34} \div 10^{36} \text{ kg/kpc}^3$. For any cluster obeying the condition chosen for the mass ratio gal-to-gas, we assume a typical elliptical and cD galaxy mass in the range $10^{12} \div 10^{13} M_\odot$.
- the constant $\rho_{gal,2}$ has been fixed with the only requirement that the galaxy density function has to be continuous at R_c .

We have tested the effect of varying galaxy density in the above range $\sim 10^{34} \div 10^{36} \text{ kg/kpc}^3$ on the cluster with the lowest mass, namely A262. In this case, we would expect great variations with respect to other clusters; the result is that the contribution due to galaxies and cD-galaxy gives a variation $\leq 1\%$ to the final estimate of fit parameters. The cD galaxy density has been modelled as described in (Schmidt 2006); they use a Jaffe model of the form:

$$\rho_{CDgal} = \frac{\rho_{0,J}}{\left(\frac{r}{r_c}\right)^2 \left(1 + \frac{r}{r_c}\right)^2} \quad (39)$$

where r_c is the core radius while the central density is obtained from $M_J = \frac{4}{3} \pi R_c^3 \rho_{0,J}$. The mass of the cD galaxy has been fixed at $1.14 \times 10^{12} M_\odot$, with $r_c = R_e/0.76$, with $R_e = 25$ kpc being the effective radius of the galaxy. The central galaxy for each cluster in the sample is assumed to have approximately this stellar mass.

Table 1. Column 1: Cluster name. Column2: Richness. Column 3: cluster total mass. Column 4: gas mass. Column 5: galaxy mass. Column 6: cD-galaxy mass. Gas and total mass values are estimated at $r = r_{max}$. Column 7: ratio of total galaxy mass to gas mass. Column 8: minimum radius. Column 9: maximum radius.

name	R	$M_{cl,N}$ (M_{\odot})	M_{gas} (M_{\odot})	M_{gal} (M_{\odot})	M_{cDgal} (M_{\odot})	$\frac{gal}{gas}$	r_{min} (kpc)	r_{max} (kpc)
A133	0	$4.35874 \cdot 10^{14}$	$2.73866 \cdot 10^{13}$	$5.20269 \cdot 10^{12}$	$1.10568 \cdot 10^{12}$	0.23	86	1060
A262	0	$4.45081 \cdot 10^{13}$	$2.76659 \cdot 10^{12}$	$1.71305 \cdot 10^{11}$	$5.16382 \cdot 10^{12}$	0.25	61	316
A383	2	$2.79785 \cdot 10^{14}$	$2.82467 \cdot 10^{13}$	$5.88048 \cdot 10^{12}$	$1.09217 \cdot 10^{12}$	0.25	52	751
A478	2	$8.51832 \cdot 10^{14}$	$1.05583 \cdot 10^{14}$	$2.15567 \cdot 10^{13}$	$1.67513 \cdot 10^{12}$	0.22	59	1580
A907	1	$4.87657 \cdot 10^{14}$	$6.38070 \cdot 10^{13}$	$1.34129 \cdot 10^{13}$	$1.66533 \cdot 10^{12}$	0.24	563	1226
A1413	3	$1.09598 \cdot 10^{15}$	$9.32466 \cdot 10^{13}$	$2.30728 \cdot 10^{13}$	$1.67345 \cdot 10^{12}$	0.26	57	1506
A1795	2	$5.44761 \cdot 10^{14}$	$5.56245 \cdot 10^{13}$	$4.23211 \cdot 10^{12}$	$1.93957 \cdot 10^{12}$	0.11	79	1151
A1991	1	$1.24313 \cdot 10^{14}$	$1.00530 \cdot 10^{13}$	$1.24608 \cdot 10^{12}$	$1.08241 \cdot 10^{12}$	0.23	55	618
A2029	2	$8.92392 \cdot 10^{14}$	$1.24129 \cdot 10^{14}$	$3.21543 \cdot 10^{13}$	$1.11921 \cdot 10^{12}$	0.27	62	1771
A2390	1	$2.09710 \cdot 10^{15}$	$2.15726 \cdot 10^{14}$	$4.91580 \cdot 10^{13}$	$1.12141 \cdot 10^{12}$	0.23	83	1984
MKW4	-	$4.69503 \cdot 10^{13}$	$2.83207 \cdot 10^{12}$	$1.71153 \cdot 10^{11}$	$5.29855 \cdot 10^{11}$	0.25	60	434
RXJ1159	-	$8.97997 \cdot 10^{13}$	$4.33256 \cdot 10^{12}$	$7.34414 \cdot 10^{11}$	$5.38799 \cdot 10^{11}$	0.29	64	568

We have assumed that the total galaxy-component mass (galaxies plus cD galaxy masses) is $\approx 20 \div 25\%$ of the gas mass: in (Schindler 2004), the mean fraction of gas versus the total mass (with dark matter) for a cluster is estimated to be $15 \div 20\%$, while the same quantity for galaxies is $3 \div 5\%$. This means that the relative mean mass ratio gal-to-gas in a cluster is $\approx 20 \div 25\%$. We have varied the parameters $\rho_{gal,1}$, $\rho_{gal,2}$ and M_J in their previous defined ranges to obtain a mass ratio between total galaxy mass and total gas mass which lies in this range. Resulting galaxy mass values and ratios $\frac{gal}{gas}$, estimated at $r = r_{max}$, are listed in Table 1.

In Fig. (1), we show how each component is spatially distributed. The CD-galaxy is dominant with respect to the other galaxies only in the inner region (below 100 kpc). As already stated in § 5.1, cluster innermost regions have been excluded from our analysis and so the contribution due to the cD-galaxy is practically negligible in our analysis. The gas is, as a consequence, clearly the dominant visible component, starting from innermost regions out to large radii, being galaxy mass only $20 \div 25\%$ of gas mass. A similar behavior is shown by all the clusters considered in our sample.

5.4 Uncertainties on mass profiles

Uncertainties on the cluster total mass profiles have been estimated performing Monte-Carlo simulations (Neumann 1995). We proceed to simulate temperature profiles and choose random radius-temperature values couples for each bin which we have in our temperature data given by (Vikhlinin et al.2005). Random temperature values have been extracted from a Gaussian distribution centered on the spectral values, and with a dispersion fixed to its 68% confidence level. For the radius, we choose a random value inside each bin. We have performed 2000 simulations for each cluster and perform two cuts on the simulated profile. First, we exclude those profiles that give an unphysical negative estimate of the mass: this is possible when our simulated couples of quantities give rise to too high temperature-gradient. After this cut, we have ≈ 1500 simulations for any cluster. Then we have ordered the resulting mass values for increasing radius values. Extreme mass estimates (outside

the $10 \div 90\%$ range) are excluded from the obtained distribution, in order to avoid other high mass gradients which give rise to masses too different from real data. The resulting limits provide the errors on the total mass. Uncertainties on the electron-density profiles have not been included in the simulations, being them negligible with respect to those of the gas-temperature profiles.

5.5 Fitting the mass profiles

In the above sections, we have shown that, with the aid of X-ray observations, modelling theoretically the galaxy distribution and using Eq. (33), we obtain an estimate of the baryonic content of clusters.

We have hence performed a best-fit analysis of the theoretical Eq. (33)

$$M_{bar,theo}(r) = \frac{4a_1}{3} \left[-\frac{kT(r)}{\mu m_p G} r \left(\frac{d \ln \rho_{gas}(r)}{d \ln r} + \frac{d \ln T(r)}{d \ln r} \right) \right] + \frac{4a_1}{3G} r^2 \frac{d\Phi_C}{dr}(r) \quad (40)$$

versus the observed mass contributions

$$M_{bar,obs}(r) = M_{gas}(r) + M_{gal}(r) + M_{cDgal}(r) \quad (41)$$

Since not all the data involved in the above estimate have measurable errors, we cannot perform an *exact* χ -square minimization: Actually, we can minimize the quantity:

$$\chi^2 = \frac{1}{N - n_p - 1} \cdot \sum_{i=1}^N \frac{(M_{bar,obs} - M_{bar,theo})^2}{M_{bar,theo}} \quad (42)$$

where N is the number of data and $n_p = 2$ the free parameters of the model. We minimize the χ -square using the Markov Chain Monte Carlo Method (MCMC). For each cluster, we have run various chains to set the best parameters of the used algorithm, the Metropolis-Hastings one: starting from an initial parameter vector \mathbf{p} (in our case $\mathbf{p} = (a_1, a_2)$), we generate a new trial point \mathbf{p}' from a tested proposal density $q(\mathbf{p}', \mathbf{p})$, which represents the conditional probability to get \mathbf{p}' , given \mathbf{p} . This new point is accepted with probability

Table 2. Column 1: Cluster name. Column 2: first derivative coefficient, a_1 , of $f(R)$ series. Column3: 1σ confidence interval for a_1 . Column 4: second derivative coefficient, a_2 , of $f(R)$ series. Column 5: 1σ confidence interval for a_2 . Column 6: characteristic length, L , of the modified gravitational potential, derived from a_1 and a_2 . Column 7 : 1σ confidence interval for L .

name	a_1	$[a_1 - 1\sigma, a_1 + 1\sigma]$	a_2 (kpc ²)	$[a_2 - 1\sigma, a_2 + 1\sigma]$ (kpc ²)	L (kpc)	$[L - 1\sigma, L + 1\sigma]$ (kpc)
A133	0.085	[0.078, 0.091]	$-4.98 \cdot 10^3$	$[-2.38 \cdot 10^4, -1.38 \cdot 10^3]$	591.78	[323.34, 1259.50]
A262	0.065	[0.061, 0.071]	-10.63	[-57.65, -3.17]	31.40	[17.28, 71.10]
A383	0.099	[0.093, 0.108]	$-9.01 \cdot 10^2$	$[-4.10 \cdot 10^3, -3.14 \cdot 10^2]$	234.13	[142.10, 478.06]
A478	0.117	[0.114, 0.122]	$-4.61 \cdot 10^3$	$[-1.01 \cdot 10^4, -2.51 \cdot 10^3]$	484.83	[363.29, 707.73]
A907	0.129	[0.125, 0.136]	$-5.77 \cdot 10^3$	$[-1.54 \cdot 10^4, -2.83 \cdot 10^3]$	517.30	[368.84, 825.00]
A1413	0.115	[0.110, 0.119]	$-9.45 \cdot 10^4$	$[-4.26 \cdot 10^5, -3.46 \cdot 10^4]$	2224.57	[1365.40, 4681.21]
A1795	0.093	[0.084, 0.103]	$-1.54 \cdot 10^3$	$[-1.01 \cdot 10^4, -2.49 \cdot 10^2]$	315.44	[133.31, 769.17]
A1991	0.074	[0.072, 0.081]	-50.69	$[-3.42 \cdot 10^2, -13]$	64.00	[32.63, 159.40]
A2029	0.129	[0.123, 0.134]	$-2.10 \cdot 10^4$	$[-7.95 \cdot 10^4, -8.44 \cdot 10^3]$	988.85	[637.71, 1890.07]
A2390	0.149	[0.146, 0.152]	$-1.40 \cdot 10^6$	$[-5.71 \cdot 10^6, -4.46 \cdot 10^5]$	7490.80	[4245.74, 15715.60]
MKW4	0.054	[0.049, 0.060]	-23.63	$[-1.15 \cdot 10^2, -8.13]$	51.31	[30.44, 110.68]
RXJ1159	0.048	[0.047, 0.052]	-18.33	$[-1.35 \cdot 10^2, -4.18]$	47.72	[22.86, 125.96]

$$\alpha(\mathbf{p}, \mathbf{p}') = \min \left\{ 1, \frac{L(\mathbf{d}|\mathbf{p}')P(\mathbf{p}')q(\mathbf{p}', \mathbf{p})}{L(\mathbf{d}|\mathbf{p})P(\mathbf{p})q(\mathbf{p}, \mathbf{p}')} \right\}$$

where \mathbf{d} are the data, $L(\mathbf{d}|\mathbf{p}') \propto \exp(-\chi^2/2)$ is the likelihood function, $P(\mathbf{p})$ is the prior on the parameters. In our case, the prior on the fit parameters is related to Eq. (13): being L a length, we need to force the ratio a_1/a_2 to be positive. The proposal density is Gaussian symmetric with respect of the two vectors \mathbf{p} and \mathbf{p}' , namely $q(\mathbf{p}, \mathbf{p}') \propto \exp(-\Delta\mathbf{p}^2/2\sigma^2)$, with $\Delta\mathbf{p} = \mathbf{p} - \mathbf{p}'$; we decide to fix the dispersion σ of any trial distribution of parameters equal to 20% of trial a_1 and a_2 at any step. This means that the parameter α reduces to the ratio between the likelihood functions. We have run one chain of 10^5 points for every cluster; the convergence of the chains has been tested using the power spectrum analysis from (Dunkley 2005). The key idea of this method is, at the same time, simple and powerful: if we take the *power spectra* of the MCMC samples, we will have a great correlation on small scales but, when the chain reaches convergence, the spectrum becomes flat (like a white noise spectrum); so that, by checking the spectrum of just one chain (instead of many parallel chains as in Gelmann-Rubin test) will be sufficient to assess the reached convergence. Remanding to (Dunkley 2005) for a detailed discussion of all the mathematical steps. Here we calculate the discrete power spectrum of the chains:

$$P_j = |a_N^j|^2 \quad (43)$$

with

$$a_N^j = \frac{1}{\sqrt{N}} \sum_{n=0}^{N-1} x_n \exp \left[i \frac{2\pi j}{N} n \right] \quad (44)$$

where N and x_n are the length and the element of the sample from the MCMC, respectively, $j = 1, \dots, \frac{N}{2} - 1$. The wavenumber k_j of the spectrum is related to the index j by the relation $k_j = \frac{2\pi j}{N}$. Then we fit it with the analytical template:

$$P(k) = P_0 \frac{(k^*/k)^\alpha}{1 + (k^*/k)^\alpha} \quad (45)$$

or in the equivalent logarithmic form:

$$\ln P_j = \ln P_0 + \ln \left[\frac{(k^*/k_j)^\alpha}{1 + (k^*/k_j)^\alpha} \right] - \gamma + r_j \quad (46)$$

where $\gamma = 0.57216$ is the Euler-Mascheroni number and r_j are random measurement errors with $\langle r_j \rangle = 0$ and $\langle r_i r_j \rangle = \delta_{ij} \pi^2/6$. From the fit, we estimate the two fundamental parameters, P_0 and j^* (the index corresponding to k^*). The first one is the value of the power spectrum extrapolated for $k \rightarrow 0$ and, from it, we can derive the convergence ratio from $r \approx \frac{P_0}{N}$; if $r < 0.01$, we can assume that the convergence is reached. The second parameter is related to the turning point from a power-law to a flat spectrum. It has to be > 20 in order to be sure that the number of points in the sample, coming from the convergence region, are more than the noise points. If these two conditions are verified for all the parameters, then the chain has reached the convergence and the statistics derived from MCMC well describes the underlying probability distribution (typical results are shown in Figs. 3, 4, 5. Following (Dunkley 2005) prescriptions, we perform the fit over the range $1 \leq j \leq j_{max}$, with $j_{max} \sim 10j^*$, where a first estimation of j^* can be obtained from a fit with $j_{max} = 1000$, and then performing a second iteration in order to have a better estimation of it. Even if the convergence is achieved after few thousand steps of the chain, we have decided to run longer chains of 10^5 points to reduce the noise from the histograms and avoid under- or over- estimations of errors on the parameters. The $i - \sigma$ confidence levels are easily estimated deriving them from the final sample the 15.87-th and 84.13-th quantiles (which define the 68% confidence interval) for $i = 1$, the 2.28-th and 97.72-th quantiles (which define the 95% confidence interval) for $i = 2$ and the 0.13-th and 99.87-th quantiles (which define the 99% confidence interval) for $i = 3$.

After the description of the method, let us now comment on the achieved results.

6 RESULTS

The numerical results of our fitting analysis are summarized in Table 2; we give the best fit values of the independent fitting parameters a_1 and a_2 , and of the gravitational

length L , considered as a function of the previous two quantities. In Figs. 3- 5, we give the typical results of fitting, with histograms and power spectrum of samples derived by the MCMC, to assess the reached convergence (flat spectrum at large scales).

The goodness and the properties of the fits are shown in Figs. 6- 17. The main property of our results is the presence of a *typical scale* for each cluster above which our model works really well (typical relative differences are less than 5%), while for lower scale there is a great difference. It is possible to see, by a rapid inspection, that this turning-point is located at a radius ≈ 150 kpc. Except for extremely rich clusters, it is clear that this value is independent of the cluster, being similar for all clusters in our sample.

There are two main independent explanations that could justify this trend: limits due to a break in the state of hydrostatic equilibrium or limits in the series expansion of the $f(R)$ -models.

If the hypothesis of hydrostatic equilibrium is not correct, then we are in a regime where the fundamental relations Eqs. (23)- (28), are not working. As discussed in (Vikhlinin et al.2005), the central (70 kpc) region of most clusters is strongly affected by radiative cooling and thus its physical properties cannot directly be related to the depth of the cluster potential well. This means that, in this region, the gas is not in hydrostatic equilibrium but in a multi-phase state. In this case, the gas temperature cannot be used as a good standard tracer.

We have also to consider another limit of our modelling: the requirement that the $f(R)$ -function is Taylor expandable. The corrected gravitational potential which we have considered is derived in the weak field limit, which means

$$R - R_0 \ll \frac{a_1}{a_2} \quad (47)$$

where R_0 is the background value of the curvature. If this condition is not satisfied, the approach does not work (see (Capozziello, Stabile and Troisi 2008a) for a detailed discussion of this point). Considering that a_1/a_2 has the dimension of $length^{-2}$ this condition defines the *length scale* where our series approximation can work. In other words, this indicates the limit in which the model can be compared with data.

For the considered sample, the fit of the parameters a_1 and a_2 , spans the length range {19; 200} kpc (except for the richest clusters). It is evident that every galaxy cluster has a *proper* gravitational length scale. It is worth noticing that a similar situation, but at completely different scales, has been found out for low surface brightness galaxies modelled by $f(R)$ -gravity (Capozziello, Cardone and Troisi 2007).

Considering the data at our disposal and the analysis which we have performed, it is not possible to quantify exactly the quantitative amount of these two different phenomena (i.e. the radiative cooling and the validity of the weak field limit). However, they are not mutually exclusive but should be considered in details in view of a more refined modelling [†].

[†] Other secondary phenomena as cooling flows, merger and asymmetric shapes have to be considered in view of a detailed modelling of clusters. However, in this work, we are only interested to show that extended gravity could be a valid alternative to dark matter in order to explain the cluster dynamics.

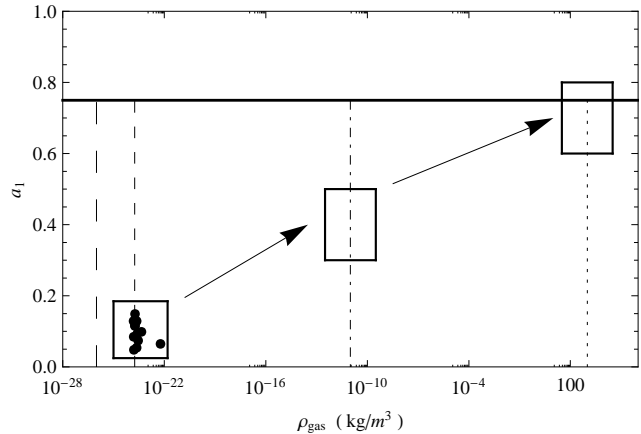


Figure 2. Density vs a_1 : predictions on the behavior of a_1 . The horizontal black bold line indicates the Newtonian-limit, $a_1 \rightarrow 3/4$ which we expect to be realized on scales comparable with Solar System. Vertical lines indicate typical approximated values of matter density (without dark matter) for different gravitational structures: universe (large dashed) with critical density $\rho_{crit} \approx 10^{-26}$ kg/m³; galaxy clusters (short dashed) with $\rho_{cl} \approx 10^{-23}$ kg/m³; galaxies (dot-dashed) with $\rho_{gal} \approx 10^{-11}$ kg/m³; sun (dotted) with $\rho_{sun} \approx 10^3$ kg/m³. Arrows and boxes show the predicted trend for a_1 .

Similar issues are present also in (Brownstein 2006B): they use the the Metric - Skew - Tensor - Gravity (MSTG) as a generalization of the Einstein General Relativity and derive the gas mass profile of a sample of clusters with gas being the only baryonic component of the clusters. They consider some clusters included in our sample (in particular, A133, A262, A478, A1413, A1795, A2029, MKW4) and they find the same different trend for $r \leq 200$ kpc, even if with a different behavior with respect to us: our model gives lower values than X-ray gas mass data while their model gives higher values with respect to X-ray gas mass data. This stresses the need for a more accurate modelling of the gravitational potential.

However, our goal is to show that potential (12) is suitable to fit the mass profile of galaxy clusters and that it comes from a self-consistent theory.

In general, it can be shown that the weak field limit of extended theories of gravity has Yukawa-like corrections (Stelle 1978; Kenmoku, Okamoto and Shigemoto1993). Specifically, given theory of gravity of order $(2n + 2)$, the Yukawa corrections to the Newtonian potential are n (Quandt 1991). This means that if the effective Lagrangian of the theory is

$$\mathcal{L} = f(R, \square R, \dots \square^k R, \dots \square^n R) \sqrt{-g} \quad (48)$$

we have

$$\phi(r) = -\frac{GM}{r} \left[1 + \sum_{k=1}^n \alpha_k e^{-r/L_k} \right]. \quad (49)$$

Standard General Relativity, where Yukawa corrections are not present, is recovered for $n = 0$ (second order theory) while the $f(R)$ -gravity is obtained for $n = 1$ (fourth-order theory). Any \square operator introduces two further derivation orders in the field equations. This kind of Lagrangian comes

out when quantum field theory is formulated on curved spacetime (Birrell & Davies1982). In the series (49), G is the value of the gravitational constant considered at infinity, L_k is the interaction length of the k -th component of the non-Newtonian corrections. The amplitude α_k of each component is normalized to the standard Newtonian term; the sign of α_k tells us if the corrections are attractive or repulsive (see (Will1993) for details). Moreover, the variation of the gravitational coupling is involved. In our case, we are taking into account only the first term of the series. It is the the leading term. Let us rewrite (12) as

$$\phi(r) = -\frac{GM}{r} \left[1 + \alpha_1 e^{-r/L_1} \right]. \quad (50)$$

The effect of non-Newtonian term can be parameterized by $\{\alpha_1, L_1\}$ which could be a useful parameterisation which respect to our previous $\{a_1, a_2\}$ or $\{G_{eff}, L\}$ with $G_{eff} = 3G/(4a_1)$. For large distances, where $r \gg L_1$, the exponential term vanishes and the gravitational coupling is G . If $r \ll L_1$, the exponential becomes 1 and, by differentiating Eq.(50) and comparing with the gravitational force measured in laboratory, we get

$$G_{lab} = G \left[1 + \alpha_1 \left(1 + \frac{r}{L_1} \right) e^{-r/L_1} \right] \simeq G(1 + \alpha_1), \quad (51)$$

where $G_{lab} = 6.67 \times 10^{-8} \text{ g}^{-1} \text{ cm}^3 \text{ s}^{-2}$ is the usual Newton constant measured by Cavendish-like experiments. Of course, G and G_{lab} coincide in the standard Newtonian gravity. It is worth noticing that, asymptotically, the inverse square law holds but the measured coupling constant differs by a factor $(1 + \alpha_1)$. In general, any correction introduces a characteristic length that acts at a certain scale for the self-gravitating systems as in the case of galaxy cluster which we are examining here. The range of L_k of the k th-component of non-Newtonian force can be identified with the mass m_k of a pseudo-particle whose effective Compton's length can be defined as

$$L_k = \frac{\hbar}{m_k c}. \quad (52)$$

The interpretation of this fact is that, in the weak energy limit, fundamental theories which attempt to unify gravity with the other forces introduce, in addition to the massless graviton, particles *with mass* which also carry the gravitational interaction (Gibbons & Whiting1981). See, in particular, (Capozziello et al.2008b) for $f(R)$ -gravity. These masses are related to effective length scales which can be parameterized as

$$L_k = 2 \times 10^{-5} \left(\frac{1 \text{ eV}}{m_k} \right) \text{ cm}. \quad (53)$$

There have been several attempts to experimentally constrain L_k and α_k (and then m_k) by experiments on scales in the range $1 \text{ cm} < r < 1000 \text{ km}$, using different techniques (Fischbach et al. 1986; Speake & Quinn1988; Eckhardt1993). In this case, the expected masses of particles which should carry the additional gravitational force are in the range $10^{-13} \text{ eV} < m_k < 10^{-5} \text{ eV}$. The general outcome of these experiments, even retaining only the term $k = 1$, is that *geophysical window* between the laboratory and the astronomical scales has to be taken into account. In fact, the range

$$|\alpha_1| \sim 10^{-2}, \quad L_1 \sim 10^2 \div 10^3 \text{ m}, \quad (54)$$

is not excluded at all in this window. An interesting suggestion has been given by Fujii (Fujii1988), which proposed that the exponential deviation from the Newtonian standard potential could arise from the microscopic interaction which couples the nuclear isospin and the baryon number.

The astrophysical counterparts of these non-Newtonian corrections seemed ruled out till some years ago due to the fact that experimental tests of General Relativity seemed to predict the Newtonian potential in the weak energy limit, "inside" the Solar System. However, as it has been shown, several alternative theories seem to evade the Solar System constraints (see (Capozziello et al.2008b) and the reference therein for recent results) and, furthermore, indications of an anomalous, long-range acceleration revealed from the data analysis of Pioneer 10/11, Galileo, and Ulysses spacecrafts (which are now almost outside the Solar System) makes these Yukawa-like corrections come again into play (Anderson et al.1998). Besides, it is possible to reproduce phenomenologically the flat rotation curves of spiral galaxies considering the values

$$\alpha_1 = -0.92, \quad L_1 \sim 40 \text{ kpc}. \quad (55)$$

The main hypothesis of this approach is that the additional gravitational interaction is carried by some ultra-soft boson whose range of mass is $m_1 \sim 10^{-27} \div 10^{-28} \text{ eV}$. The action of this boson becomes efficient at galactic scales without the request of enormous amounts of dark matter to stabilize the systems (Sanders1990).

Furthermore, it is possible to use a combination of two exponential correction terms and give a detailed explanation of the kinematics of galaxies and galaxy clusters, again without dark matter model (Eckhardt1993).

It is worthwhile to note that both the spacecrafts measurements and galactic rotation curves indications come from "outside" the usual Solar System boundaries used up to now to test General Relativity. However, the above results *do not come* from any fundamental theory to explain the outcome of Yukawa corrections. In their contexts, these terms are phenomenological.

Another important remark in this direction deserves the fact that some authors (McGaugh2000) interpret also the experiments on cosmic microwave background like the experiment BOOMERANG and WMAP (de Bernardis et al. 2000; Spergel et al. 2003) in the framework of *modified Newtonian dynamics* again without invoking any dark matter model.

All these facts point towards the line of thinking that also corrections to the standard gravity have to be seriously taken into account beside dark matter searches.

In our case, the parameters $a_{1,2}$, which determine the gravitational correction and the gravitational coupling, come out "directly" from a field theory with the only requirement that the effective action of gravity could be more general than the Hilbert-Einstein theory $f(R) = R$. This main hypothesis comes from fundamental physics motivations due to the fact that any unification scheme or quantum field theory on curved space have to take into account higher order terms in curvature invariants (Birrell & Davies1982). Besides, several recent results point out that such corrections have a main role also at astrophysical and cosmological scales. For a detailed discussion, see (Nojiri & Odintsov 2007; Capozziello & Francaviglia 2008; Sotiriou & Faraoni2008).

With this philosophy in mind, we have plotted the trend of a_1 as a function of the density in Fig.2. As one can see, its values are strongly constrained in a narrow region of the parameter space, so that a_1 can be considered a "tracer" for the size of gravitational structures. The value of a_1 range between $\{0.8 \div 0.12\}$ for larger clusters and $\{0.4 \div 0.6\}$ for poorer structures (i.e. galaxy groups like MKW4 and RXJ1159). We expect a particular trend when applying the model to different gravitational structures. In Fig. 2, we give characteristic values of density which range from the biggest structure, the observed Universe (large dashed vertical line), to the smallest one, the Sun (vertical dotted line), through intermediate steps like clusters (vertical short dashed line) and galaxies (vertical dot-dashed line). The bold black horizontal line represents the Newtonian limit $a_1 = 3/4$ and the boxes indicate the possible values of a_1 that we obtain by applying our theoretical model to different structures.

Similar considerations hold also for the characteristic gravitational length L directly related to both a_1 and a_2 . The parameter a_2 shows a very large range of variation $\{-10^6 \div -10\}$ with respect to the density (and the mass) of the clusters. The value of L changes with the sizes of gravitational structure (see Fig. 18), so it can be considered, beside the Schwarzschild radius, a sort of additional gravitational radius. Particular care must be taken when considering Abell 2390, which shows large cavities in the X-ray surface brightness distribution, and whose central region, highly asymmetric, is not expected to be in hydrostatic equilibrium. All results at small and medium radii for this cluster could hence be strongly biased by these effects (Vikhlinin et al.2006); the same will hold for the resulting exceptionally high value of L . Fig. 18 shows how observational properties of the cluster, which well characterize its gravitational potential (such as the average temperature and the total cluster mass within r_{500} , plotted in the left and right panel, respectively), well correlate with the characteristic gravitational length L .

For clusters, we can define a gas-density-weighted and a gas-mass-weighted mean, both depending on the series parameters $a_{1,2}$. We have:

$$\begin{aligned} \langle L \rangle_\rho &= 318 \text{ kpc} & \langle a_2 \rangle_\rho &= -3.40 \cdot 10^4 \\ \langle L \rangle_M &= 2738 \text{ kpc} & \langle a_2 \rangle_M &= -4.15 \cdot 10^5 \end{aligned} \quad (56)$$

It is straightforward to note the correlation with the sizes of the cluster cD-dominated-central region and the "gravitational" interaction length of the whole cluster. In other words, the parameters $a_{1,2}$, directly related to the first and second derivative of a given analytic $f(R)$ -model determine the characteristic sizes of the self gravitating structures.

7 DISCUSSION AND CONCLUSIONS

In this paper we have investigated the possibility that the high observational mass-to-light ratio of galaxy clusters could be addressed by $f(R)$ -gravity without assuming huge amounts of dark matter. We point out that this proposal comes out from the fact that, up to now, no definitive candidate for dark-matter has been observed at fundamental level and then alternative solutions to the problem should be viable. Furthermore, several results in $f(R)$ -gravity seem to confirm that valid alternatives to Λ CDM can be achieved

in cosmology. Besides, as discussed in the Introduction, the rotation curves of spiral galaxies can be explained in the weak field limit of $f(R)$ -gravity. Results of our analysis go in this direction.

We have chosen a sample of relaxed galaxy clusters for which accurate spectroscopic temperature measurements and gas mass profiles are available. For the sake of simplicity, and considered the sample at our disposal, every cluster has been modelled as a self bound gravitational system with spherical symmetry and in hydrostatic equilibrium. The mass distribution has been described by a corrected gravitational potential obtained from a generic analytic $f(R)$ -theory. In fact, as soon as $f(R) \neq R$, Yukawa-like exponential corrections emerge in the weak field limit while the standard Newtonian potential is recovered only for $f(R) = R$, the Hilbert-Einstein theory.

Our goal has been to analyze if the dark-matter content of clusters can be addressed by these correction potential terms. As discussed in detail in the previous section and how it is possible to see by a rapid inspection of Figs. 6- 17, all the clusters of the sample are consistent with the proposed model at 1σ confidence level. This shows, at least *qualitatively*, that the high mass-to-light ratio of clusters can be explained by using a modified gravitational potential. The good agreement is achieved on distance scales starting from 150 kpc up to 1000 kpc. The differences observed at smaller scales can be ascribed to non-gravitational phenomena, such as cooling flows, or to the fact that the gas mass is not a good tracer at this scales. The remarkable result is that we have obtained a consistent agreement with data only using the corrected gravitational potential in a large range of radii. In order to put in evidence this trend, we have plotted the baryonic mass vs radii considering, for each cluster, the scale where the trend is clearly evident.

In our knowledge, the fact that $f(R)$ -gravity could work at these scales has been only supposed but never achieved by a direct fitting with data (see (Lobo 2008) for a review). Starting from the series coefficients a_1 and a_2 , it is possible to state that, at cluster scales, two characteristic sizes emerge from the weak field limit of the theory. However, at smaller scales, e.g. Solar System scales, standard Newtonian gravity has to be dominant in agreement with observations.

In conclusion, if our considerations are right, gravitational interaction depends on the scale and the *infrared limit* is led by the series coefficient of the considered effective gravitational Lagrangian. Roughly speaking, we expect that starting from cluster scale to galaxy scale, and then down to smaller scales as Solar System or Earth, the terms of the series lead the clustering of self-gravitating systems beside other non-gravitational phenomena. In our case, the Newtonian limit is recovered for $a_1 \rightarrow 3/4$ and $L(a_1, a_2) \gg r$ at small scales and for $L(a_1, a_2) \ll r$ at large scales. In the first case, the gravitational coupling has to be redefined, in the second $G_\infty \simeq G$. In these limits, the linear Ricci term is dominant in the gravitational Lagrangian and the Newtonian gravity is restored (Quandt 1991). Reversing the argument, this could be the starting point to achieve a theory capable of explaining the strong segregation in masses and sizes of gravitationally-bound systems.

8 ACKNOWLEDGMENTS

We warmly thank V.F. Cardone for priceless help in computational work. We acknowledge A. Stabile and A. Troisi for comments, discussions and suggestions on the topic and M. Paolillo for hints and suggestions in cluster modelling. We are indebted with A. Vikhlinin which kindly gave us data on cluster temperature profiles.

REFERENCES

- Allemandi, G., Francaviglia, M., Ruggiero, M., Tartaglia, A. 2005, *Gen. Rel. Grav.*, 37, 1891
- Anderson J.D., et al., 1998, *Phys. Rev. Lett.* **81**, 2858.
- Astier, P. et al. 2006, *A&A*, 447, 31
- Bahcall N. A., 1996, in "Formation of structure in the universe, 1995, Jerusalem Winter School", astro-ph/9611148,
- Bahcall, N.A. et al. 2003, *ApJ*, 585, 182
- Bahcall, N.A., Bode, P. 2003, *ApJ*, 588, 1
- Bautz, L. P., Morgan, W. W., 1970, *ApJ*, 162, L149
- Birrell, N.D. and Davies, P.C.W., 1982, *Quantum Fields in Curved Space*, Cambridge Univ. Press, Cambridge
- Borowiec, A., Godlowski, W., Szydlowski, M. 2006, *Phys. Rev. D*, 74, 043502
- Brownstein, J. R., Moffat, J. W., 2006, *MNRAS*, 367, 527
- Capozziello, S. 2002, *Int. J. Mod. Phys. D*, 11, 483
- Capozziello, S., Cardone, V.F., Carloni, S., Troisi, A. 2003, *Int. J. Mod. Phys. D*, 12, 1969
- Capozziello, S., Cardone, V.F., Francaviglia, M. 2006, *Gen. Rel. Grav.*, 38, 711
- Capozziello, S., Cardone, V.F., Troisi, A. 2005, *Phys. Rev. D*, 71, 043503
- Capozziello, S., Cardone, V.F., Troisi, A. 2006, *JCAP*, 0608, 001
- Capozziello, S., Cardone, V. F., Troisi, A., 2007, *MNRAS*, 375, 1423
- Capozziello, S., Stabile A., Troisi, A., 2007, *Class. quant. grav.*, 24, 2153
- Capozziello, S., Stabile, A., Troisi, A., 2008, *Physical Review D*, 76, 104019
- Capozziello, S., De Laurentis, M., Nojiri, S., Odintsov, S.D., 2008, arXiv:0808.1335 [hep-th]
- Capozziello, S., Carloni, S., Troisi, A. 2003, *Rec. Res. Devel. Astronomy. & Astrophys.*, 1, 625, astro-ph/0303041
- Capozziello S. and Francaviglia M., 2008, *Gen. Rel. Grav.: Special Issue on Dark Energy* 40, 357.
- Capozziello, S., Troisi, A. 2005, *Phys. Rev. D*, 72, 044022
- Carroll, S.M., Duvvuri, V., Trodden, M., Turner, M.S. 2004, *Phys. Rev. D*, 70, 043528
- Carroll, S.M., Press, W.H., Turner, E.L. 1992, *ARA&A*, 30, 499
- Cembranos, J.A.R. 2006, *Phys. Rev. D*, 73, 064029
- Chakrabarty, D., de Filippis, E., & Russell, H. 2008, *A&A*, 487, 75
- Chiba, T. 2003, *Phys. Lett. B*, 575, 1
- Clifton, T., Barrow, J.D. 2005, *Phys. Rev. D*, 72, 103005
- Clocchiati, A. et al. 2006, *APJ*, 642, 1
- Cole, S. et al. 2005, *MNRAS*, 362, 505
- Copeland E.J., Sami M., Tsujikawa S., 2006, *Int. Jou. Mod. Phys. D* 15, 1753
- Croft, R.A.C., Hu, W., Dave, R. 1999, *Phys. Rev. Lett.*, 83, 1092
- de Bernardis, P. et al. 2000, *Nature*, 404, 955
- de Blok, W.J.G., Bosma, A. 2002, *A&A*, 385, 816
- de Blok, W.J.G. 2005, *ApJ*, 634, 227
- De Filippis, E., Sereno, M., Bautz, Longo G., M. W., 2005, *ApJ*, 625, 108
- Dick, R. 2004, *Gen. Rel. Grav.*, 36, 217
- Dolgov, A.D., Kawasaki, M. 2003, *Phys. Lett. B*, 573, 1
- Dunkley, J., Bucher, M., Ferreira, P. G., Moodley, K., Skordis, C., 2005, *MNRAS*, 356, 925
- Eckhardt, D.H., 1993 *Phys. Rev.* **48 D**, 3762.
- Eisenstein, D. et al. 2005, *ApJ*, 633, 560
- Eke, V.R., Cole, S., Frenk, C.S., Petrick, H.J. 1998, *MNRAS*, 298, 1145
- Sotiriou, T.P. and Faraoni, V., 2008, arXiv:0805.1726 [gr-qc]
- E. Fischbach, E., Sudarsky, D., Szafer, A., Talmadge, C. and Aronson, S.H., 1986, *Phys. Rev. Lett.* **56**, 3
- Frigerio
Martins C. and Salucci P., 2007, *Mon.Not.Roy.Astron.Soc.* 381, 1103
- Y. Fujii, Y., 1988, *Phys. Lett.* **B 202**, 246
- G.W. Gibbons, G.W. and Whiting, B.F., 1981, *Nature* **291**, 636
- M. Kenmoku, M., Okamoto, Y. and Shigemoto, K., 1993, *Phys. Rev.* **48 D**, 578.
- Kluske, S., Schmidt, H.J. 1996, *Astron. Nachr.*, 37, 337
- Koivisto T., 2007, *Phys.Rev.D76*, 043527
- Lobo F.S.N., arXiv: 0807.1640[gr-qc] (2008).
- McDonald, P. et al. 2005, *ApJ*, 635, 761
- S.S. McGaugh, 2000, *Ap. J. Lett.* **541**, L33
- Mendoza S. and Rosas-Guevara Y.M., 2007, *Astron. Astrophys.* 472, 367.
- Navarro, I., van Acoleyen, K. 2005, *Phys. Lett. B*, 622, 1
- Neumann., D. M., Böhringer, H., 1995, *Astron. Astrophys.*, 301, 865
- Nojiri S. and Odintsov S.D. 2007, *Int. J. Geom. Meth. Mod. Phys.* 4, 115.
- Olmo, G.J. 2005, *Phys. Rev. D*, 72, 083505
- Padmanabhan, T. 2003, *Phys. Rept.*, 380, 235
- Peebles, P.J.E., Rathra, B. 2003, *Rev. Mod. Phys.*, 75, 559
- Pope, A.C. et al. 2005, *ApJ*, 607, 655
- Quandt, I., Schmidt H. J., 1991, *Astron. Nachr.*, 312, 97
- Refregier, A. 2003, *ARA&A*, 41, 645
- Riess, A.G. et al. 2004, *ApJ*, 607, 665
- Sahni, V., Starobinski, A. 2000, *Int. J. Mod. Phys. D*, 9, 373
- Sanchez, A.G. et al. 2006, *MNRAS*, 366, 189
- Sanders, R.H., 1990, *Ann. Rev. Astr. Ap.* **2**, 1
- Schindler, S., 2004, *Astrophys.Space Sci.*, 28, 419
- Schmidt, H.J. 2004, *Lectures on mathematical cosmology*, gr-qc/0407095
- Schmidt, R. W., Allen S. W., 2007 *MNRAS* 379, 209
- Seljak, U. et al. 2005, *Phys. Rev. D*, 71, 103515
- Sobouti, Y. 2007, *A & A*, 464, 921
- Sotiriou, T.P. 2006, *Gen. Rel. Grav.*, 38, 1407
- Speake, C.C. and Quinn, T.J., 1988, *Phys. Rev. Lett.* **61**, 1340
- Spergel, D.N. et al. 2003, *ApJS*, 148, 175
- Starobinsky, A.A. 1980, *Phys. Lett. B*, 91, 99
- Stelle, K., 1978, *Gen. Relat. Grav.*, 9, 353
- Tegmark, M. et al. 2004, *Phys. Rev. D*, 69, 103501
- van Waerbeke, L. et al. 2001, *A&A*, 374, 757
- Viana, P.T.P., Nichol, R.C., Liddle, A.R. 2002, *ApJ*, 569, 75
- Vikhlinin, A., Markevitch, M., Murray, S. S., Jones, C., Forman, W., Van Speybroeck, L., 2005, *ApJ*, 628, 655
- Vikhlinin, A., Kravtsov, A., Forman, W., Jones, C., Markevitch, M., Murray, S. S., Van Speybroeck, L., 2006, *ApJ*, 640, 691
- Will C.M., 1993, *Theory and Experiments in Gravitational Physics*, Cambridge Univ. Press, Cambridge.
- Zwicky, F., 1933, *Helv. Phys. Acta*, 6, 110

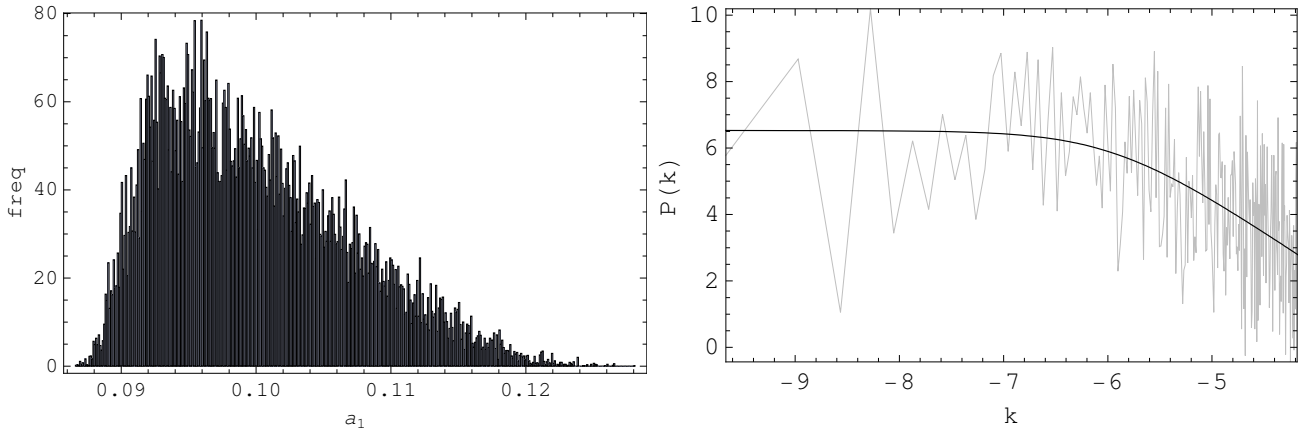


Figure 3. Left panel: histogram of the sample points for parameter a_1 in Abell 383 coming out the MCMC implementation used to estimate best fit values and errors for our fitting procedure as described in § 5.5. Binning (horizontal axis) and relative frequencies (vertical axis) are given by automatic procedure from Mathematica6.0. Right panel: power spectrum test on sample chain for parameter a_1 using the method described in § 5.5. Black line is the logarithm of the analytical template Eq. (45) for power spectrum; gray line is the discrete power spectrum obtained using Eq. (43) - (44).

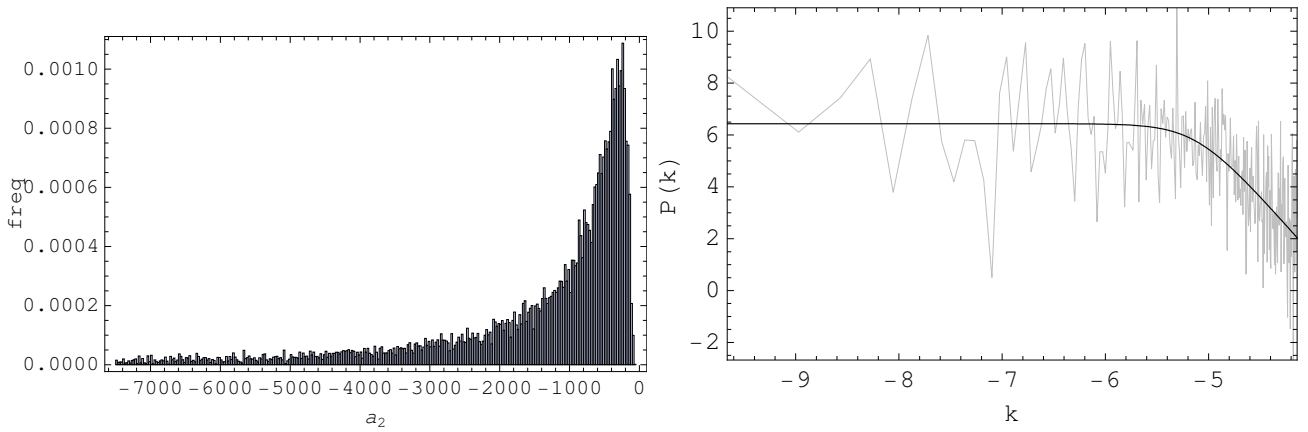


Figure 4. Abell 383: histogram (left) and power spectrum test (right) on sample chain for parameter a_2 .

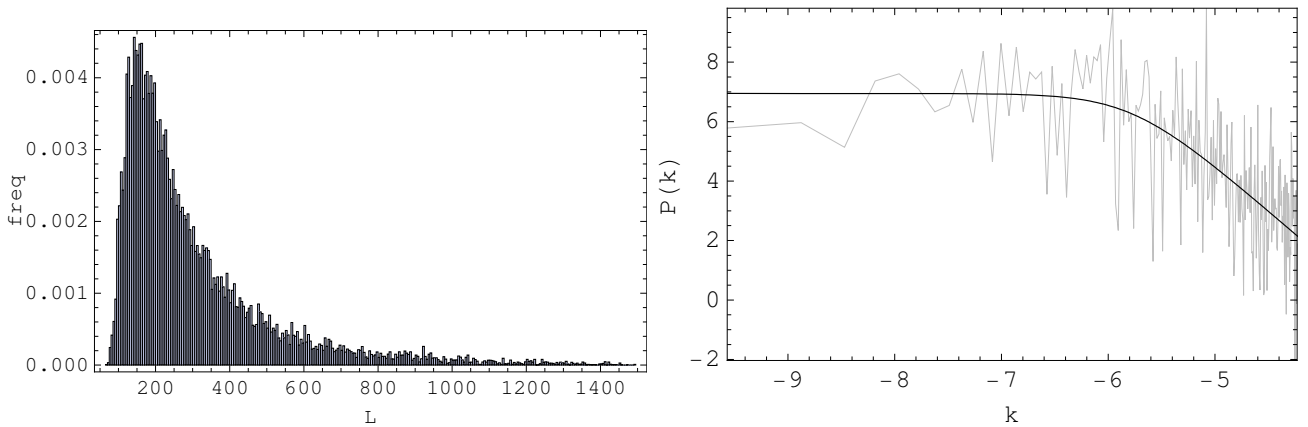


Figure 5. Abell 383: histogram (left) and power spectrum test (right) on sample chain for parameter L .

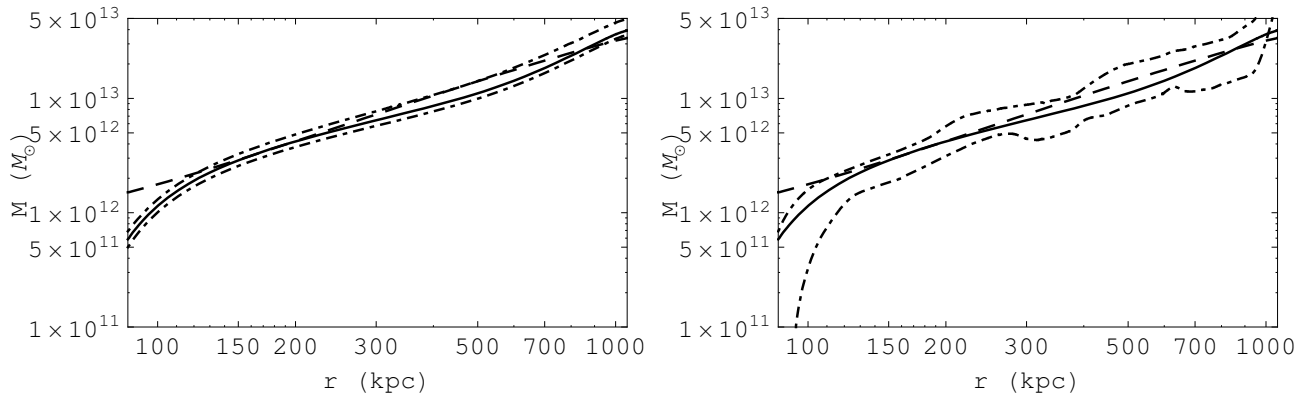


Figure 6. Baryonic mass vs radii for Abell A133. Dashed line is the experimental-observed estimation Eq. (41) of baryonic matter component (i.e. gas, galaxies and cD-galaxy); solid line is the theoretical estimation Eq. (40) for baryonic matter component. Dotted lines are the $1\text{-}\sigma$ confidence levels given by errors on fitting parameters in the left panel; and from fitting parameter plus statistical errors on mass profiles as discussed in § 5.4 in the right panel.

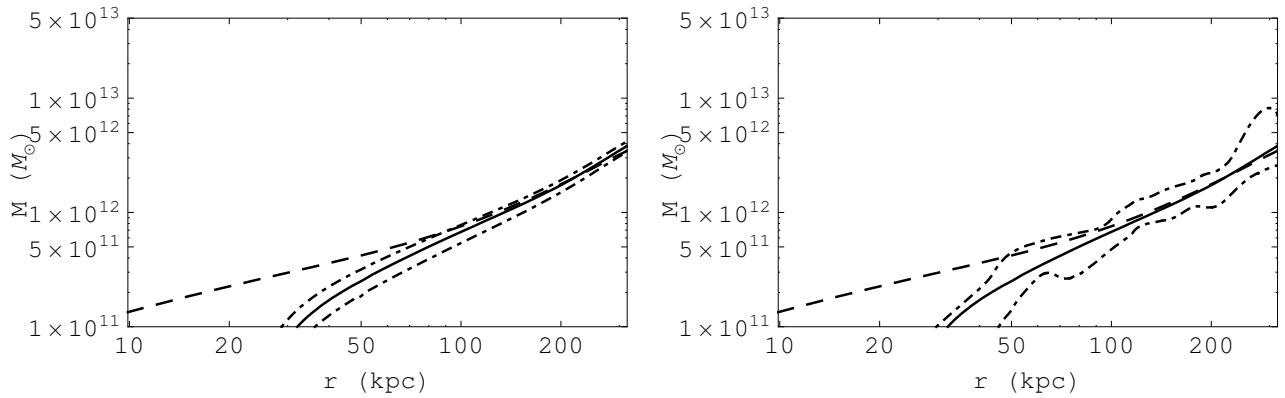


Figure 7. Same of Fig. 6 but for cluster Abell 262.

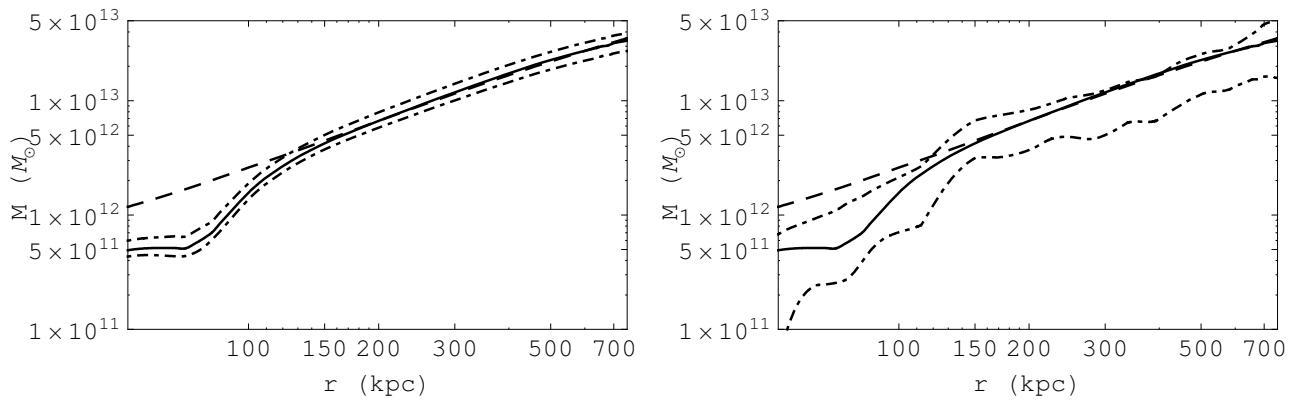


Figure 8. Same of Fig. 6 but for cluster Abell 383.

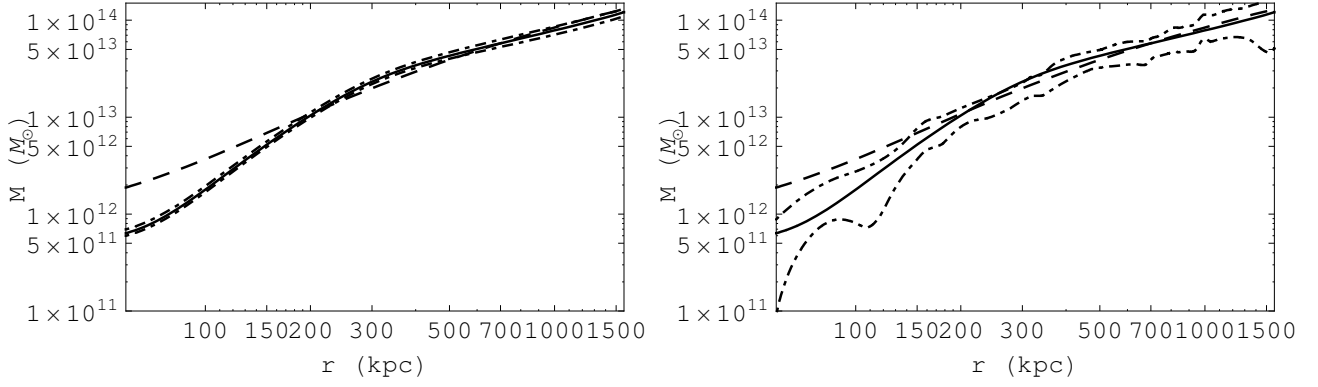


Figure 9. Same of Fig. 6 but for cluster Abell 478.

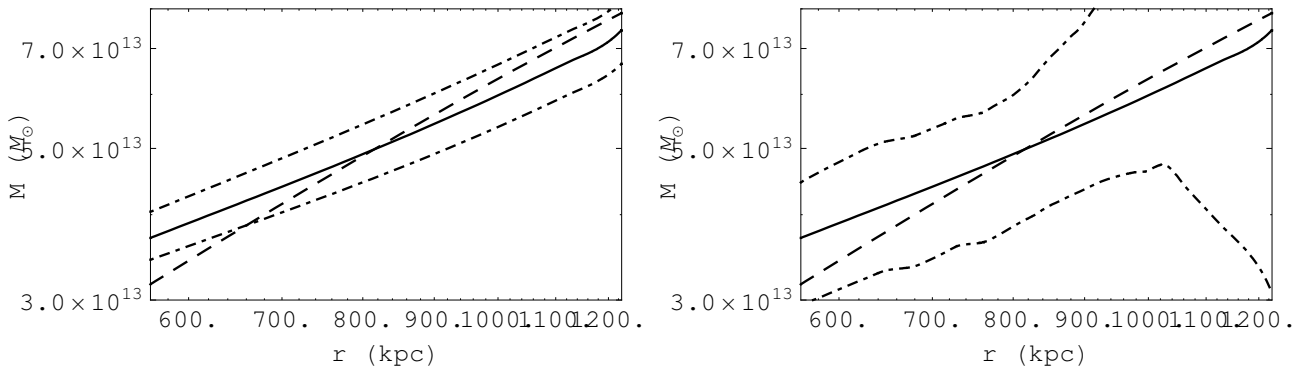


Figure 10. Same of Fig. 6 but for cluster Abell 907.

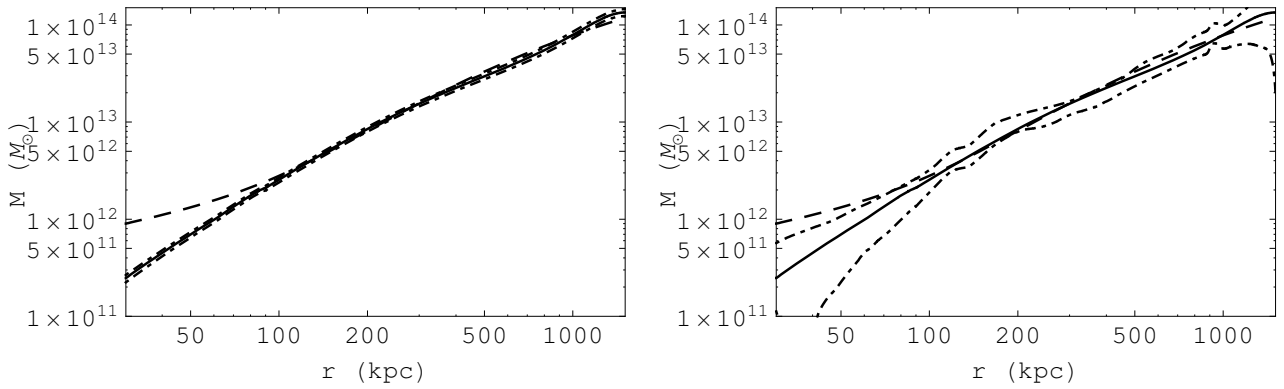


Figure 11. Same of Fig. 6 but for cluster Abell 1413.

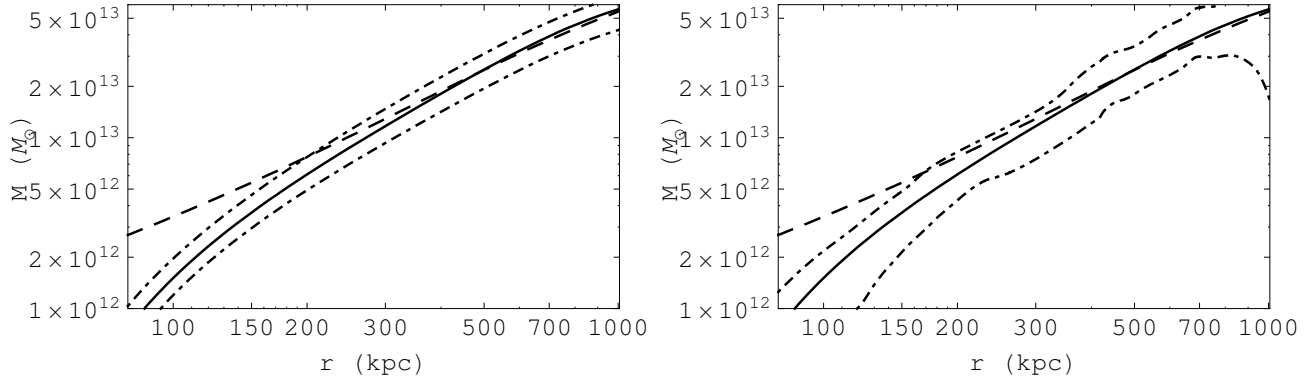


Figure 12. Same of Fig. 6 but for cluster Abell 1795.

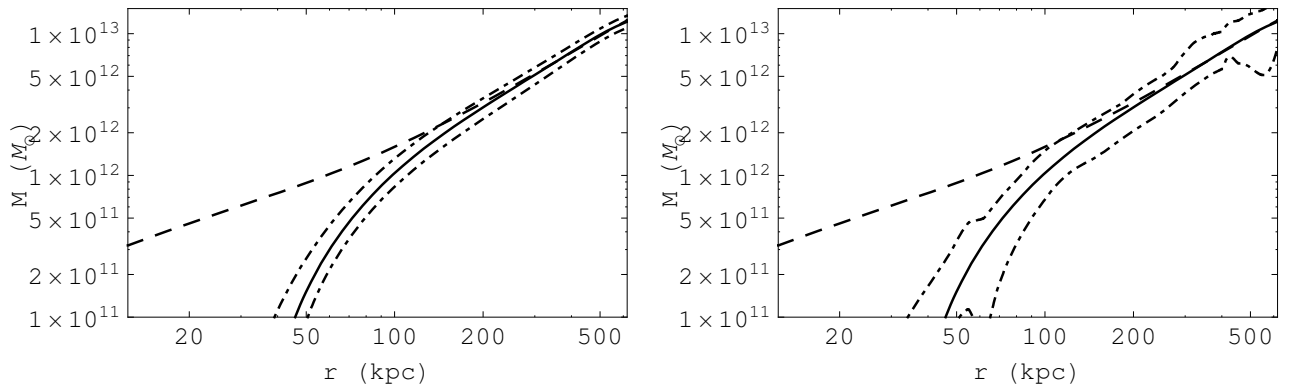


Figure 13. Same of Fig. 6 but for cluster Abell 1991.

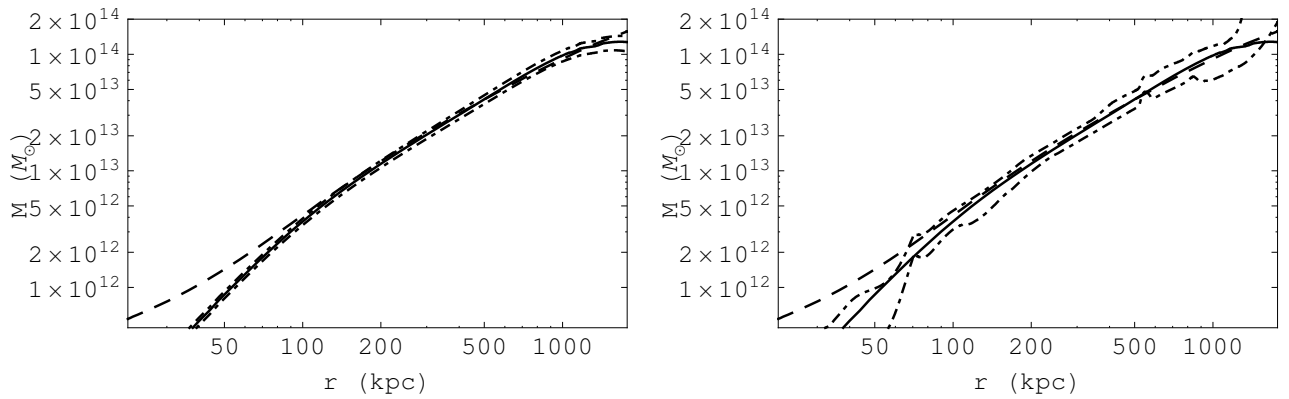


Figure 14. Same of Fig. 6 but for cluster Abell 2029.

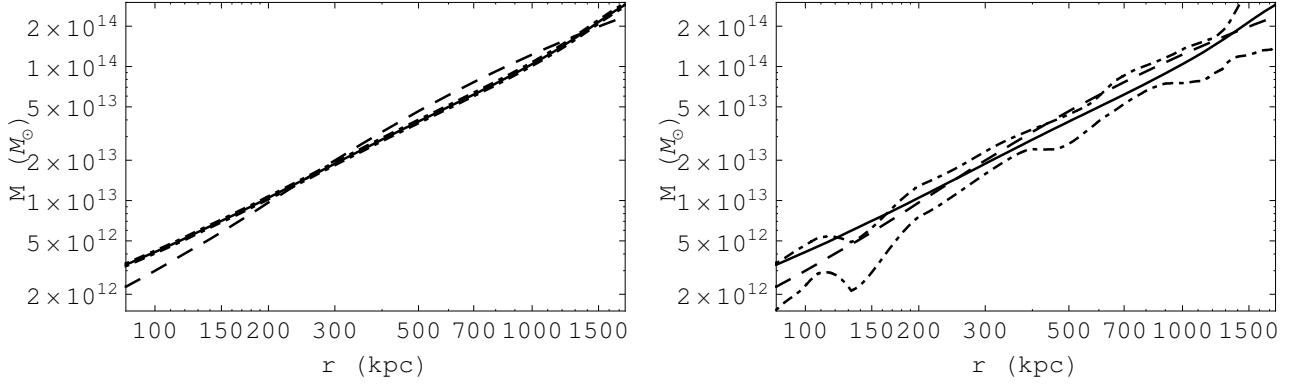


Figure 15. Same of Fig. 6 but for cluster Abell 2390.

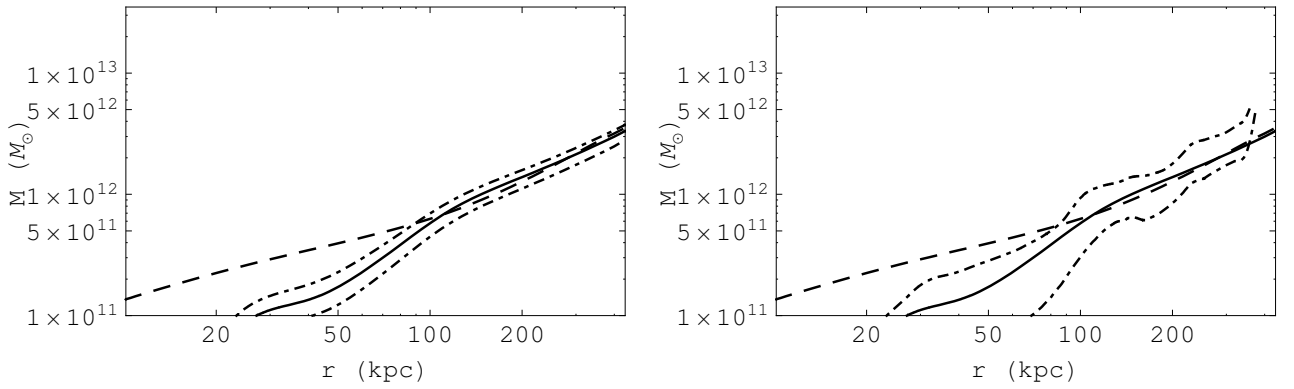


Figure 16. Same of Fig. 6 but for cluster MKW4.

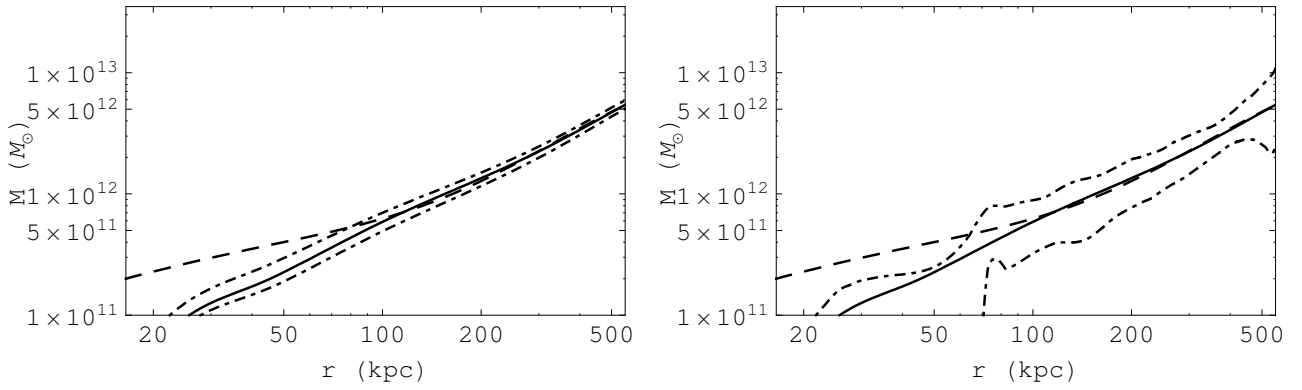


Figure 17. Same of Fig. 6 but for cluster RXJ1159.

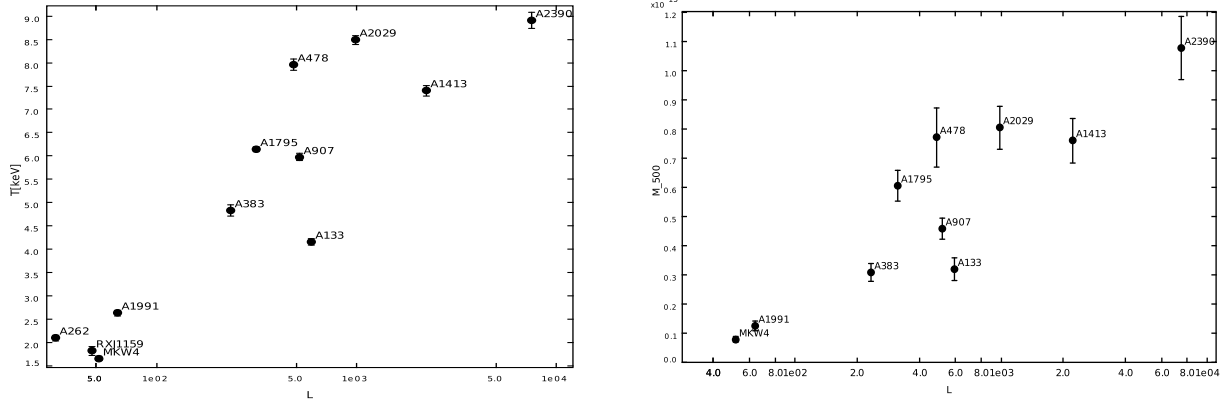


Figure 18. Single temperature fit to the total cluster spectrum (left panel) and total cluster mass within r_{500} (given as a function of M_{\odot}) (right panel) are plotted as a function of the characteristic gravitational length L . Temperature and mass values are from Vikhlinin et al.2006.